Real-Time Control of the Enantioselectivity of a Supramolecular Catalyst Allows Selecting the Configuration of Consecutively Formed Stereogenic Centers

Jeremy M Zimbron, Xavier Caumes, Yan Li, Christophe M Thomas, Matthieu Raynal, Laurent Bouteiller

Real-time control of the enantioselectivity of a supramolecular catalyst allows selecting the configuration of consecutively formed stereogenic centres

Jeremy M. Zimbron, Xavier Caumes, Yan Li, Christophe M. Thomas, Matthieu Raynal,* and Laurent Bouteiller

Abstract: The enantiomeric state of a supramolecular copper catalyst can be switched *in situ* in *ca.* five seconds. The dynamic property of the catalyst is provided by the non-covalent nature of the helical assemblies supporting the copper centres. These assemblies are formed by mixing an achiral benzene-1,3,5-tricarboxamide (BTA) phosphine ligand (for copper coordination) and both enantiomers of a chiral phosphine-free BTA co-monomer (for chirality amplification). The enantioselectivity of the hydrosilylation reaction is fixed by the BTA enantiomer in excess, which can be altered by simple BTA addition. As a result of the complete and fast stereochemical switch, any combination of the enantiomers was obtained during the conversion of a mixture of two substrates.

Dynamic and stimuli-responsive catalysts potentially allow tuning their performance during a chemical process.[1] These catalysts can be switched between different states by means of a suitable input (*i.e.* light, redox, thermal or chemical) with a significant impact on reaction rate,[1] substrate selectivity[2] or diastereoselectivity.[3] Conversely, inverting the enantioselectivity of a single catalyst during a reaction remains an elusive goal despite the promising perspectives of using such a catalyst to select the desired diastereoisomer in one pot stereoselective cascade reactions[4] or to control the tacticity of stereoblock copolymers.[5]

In fact, both enantiomers of a product can be obtained from the same catalyst[6] in a predictable manner by connecting a catalytic unit to a chiroptical switch.[7] However, the switch is commonly performed *before* the catalytic experiment.[8] Controlling the enantiomeric state of a single catalyst *in situ*[9] faces additional challenges: i) the catalytic system should be dynamic in the conditions of the catalytic reaction, ii) the stereochemical switch should be fast and lead to opposite chiral environments and, iii) the input should preserve the integrity of the catalyst. These issues are particularly significant in the case of metal-catalysed reactions since the presence of the metal centre may impede the efficiency and the dynamics of the chiroptical switch.[10] Previous attempts to switch the enantioselectivity *in situ* were also hampered by the poor stability of the metal catalysts or reactants when exposed to an oxidizing agent[9] or to ultraviolet light.[7g] Based on our previous design of catalysts supported on supramolecular helices,[11] we now describe a strategy which allows to control in real time the enantioselectivity displayed by intrinsically achiral phosphine-copper complexes located at the periphery of a chirally-amplified[12] supramolecular polymer platform. This approach relies on the complete and fast stereochemical switch of the handedness of the dynamic helices producing enantiomeric catalytic centres.

Benzene 1,3,5-tricarboxamide (BTA) monomers have been selected given their chirality amplification properties and their fast dynamics.[13] As shown in Scheme 1, we used supramolecular BTA polymers composed of three types of monomers, two enantiopure co-monomers of opposite configuration and one phosphine-functionalized achiral monomer (for copper coordination). Thanks to chirality amplification effects, homochiral helices are expected to be formed even though the polymers are composed of a scalemic mixture of enantiomers and of achiral monomers. Thus, dual stereocontrol of the asymmetric reaction should be possible by *in situ* addition of one of the enantiopure co-monomers to invert the handedness of the supramolecular helices (Scheme 1).

We chose the copper-catalysed hydrosilylation of prochiral aromatic ketones using 1-(4-nitrophenyl)ethanone (NPnone) as model substrate, because of the wide scope of reactions catalyzed by phosphine copper hydride species,[14] that include stereoselective cascade transformations.[15] We first mixed **BTA^{PPh2}** (6.0 mol%), an enantiopure BTA co-monomer (6.6 mol%) and $Cu(OAc)_2 \cdot H_2O$ (3.0 mol%) at 20°C using $PhSiH_3$ as the silane source (Table 1). We found that significant enantiomeric excesses (47%<*e.e.*<54%) were obtained with BTA co-monomers having a branched alkyl chain attached to the stereogenic centre. Notably, **BTA (*S*)-Cha** and **BTA (*R*)-Cha** provided the hydrosilylation product with opposite optical purities in a fully reproducible way (54 ±1% *e.e.*, Table S.1).

In order to implement our concept, a scalemic mixture of enantiopure co-monomers has to promote the asymmetric

[*] Dr. X. Caumes, Y. Li, Dr. M. Raynal, Dr. L. Bouteiller
Sorbonne Universités,
UPMC Univ Paris 06, CNRS,
Institut Parisien de Chimie Moléculaire,
Equipe Chimie des Polymères,
4 Place Jussieu, F-75005 Paris, France
E-mail : matthieu.raynal@upmc.fr

Dr. J. M. Zimbron, Dr. C. M. Thomas
Chimie ParisTech,
PSL Research University, CNRS,
Institut de Recherche de Chimie Paris, 75005 Paris, France.

Supporting information for this article is given via a link at the end of the document.

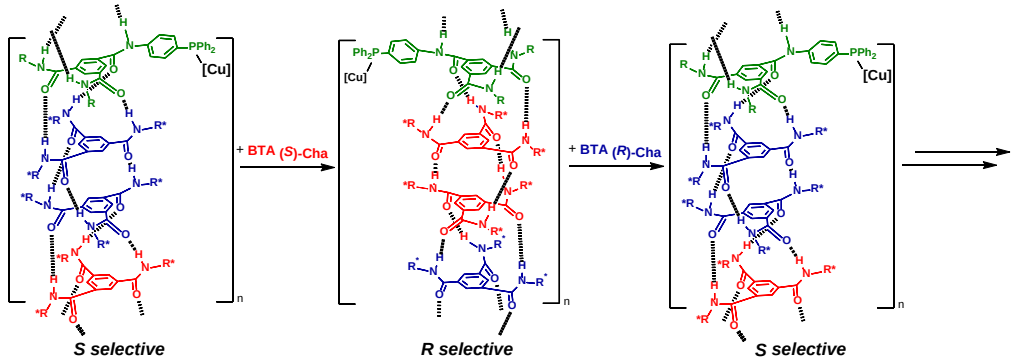

Scheme 1. Real-time control of the enantioselectivity of a supramolecular metal catalyst. The outcome of the catalytic reaction and the structure of the BTA assemblies were correlated according to various spectroscopic and scattering analyses. For the chemical structure of BTA Cha see Chart 1.

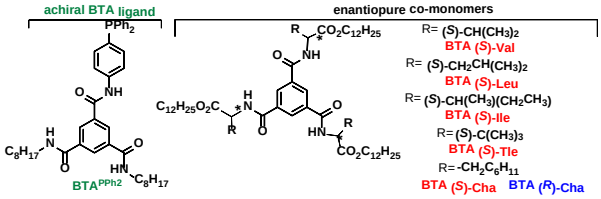

Chart 1. Chemical structures of BTA monomers screened in this study.

Table 1: Catalytic screening of BTA monomers for the copper-catalysed hydrosilylation of NPnone.[a]

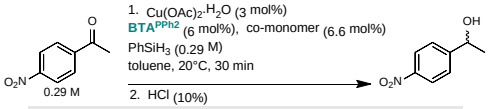

Entry	co-monomer	*e.e.* (%)
1	**BTA (*S*)-Tle**	+47 (*R*)
2	**BTA (*S*)-Val**	+48 (*R*)
3	**BTA (*S*)-Leu**	+53 (*R*)
4	**BTA (*S*)-Ile**	+53 (*R*)
5	**BTA (*S*)-Cha**	+54 (*R*)
6	**BTA (*R*)-Cha**	-54±1 (*S*)[b]

[a] Conversion>99%. [b] Based on repeatability tests (Table S.1).

reaction with a level of selectivity similar to that of the enantiopure monomer. We thus probed the selectivity obtained by mixing **BTA^{PPh2}** and a scalemic mixture of **BTA Cha** (25% *e.e.* in favour of **BTA (*R*)-Cha**) for the hydrosilylation of NPnone. Whatever the conditions probed (temperature, molar ratio of **BTA Cha** over **BTA^{PPh2}**), the enantioselectivity of the reaction remains higher than expected when considering only the optical purity of the engaged scalemic mixture (Table S.2). These chirality amplification effects are particularly strong at 20°C since a 25% *e.e.* scalemic mixture provides the product with 85% of the optimal selectivity. We further assessed the selectivity obtained for various scalemic mixtures of **BTA Cha** at 0°C (Figure 1a, blue curve). The plot displays a sigmoidal shape with a plateau, corresponding to the optimal selectivity, reached at a value of *ca.* 50% *e.e.* of **BTA Cha**. The chirality amplification is slightly decreased at this temperature since 33% *e.e.* scalemic mixtures are required to get 88% of the optimal selectivity. This reduction of the chirality amplification effect at lower temperatures has been observed previously in majority-rule experiments conducted with alkyl BTAs (see further detail in Table S.2).[16] The curve is symmetrical (inversion point at x=0): it demonstrates that the enantiomeric state of the catalyst can be inverted by simply changing the nature of the major enantiomer in the co-assemblies (*vide infra*). To further ascertain the origin of this chirality amplification effect, we precisely investigated the nature of the assemblies. When studied individually, **BTA^{PPh2}** (Figure S.1) and **BTA (*S*)-Cha** (Figure S.2) assemble into stacks[11] and dimers[17] respectively at mM concentration in toluene, in agreement with our previous results. The formation of co-assemblies between **BTA^{PPh2}** and **BTA (*S*)-Cha** ([**BTA (*S*)-Cha**]/[**BTA^{PPh2}**]=1.1) in toluene is confirmed by FT-IR (Figures S.3 and S.4) and Small Angle Neutron Scattering analyses (SANS, Figure S.5). According to a quantitative analysis of such data,[11b] the amount of **BTA (*S*)-Cha** incorporated into the stacks is ~50% meaning that *ca.* 35% of the BTA monomers present in the co-assemblies are enantiopure. The chiroptical properties of the co-assemblies were then assessed by Circular Dichroism (CD, Figure S.6).[18] All mixtures of **BTA Cha** and **BTA^{PPh2}** show a Cotton effect centred at λ=310 nm, the sign of which depends on the nature of the major enantiomer present in the co-assemblies (Figure S.7). As only **BTA^{PPh2}** absorbs in this region, the presence of this induced CD signal[19] confirms that the phosphine groups of the ligand are located in the chiral environment provided by the co-assemblies and that the direction of the induced chirality is controlled by the co-monomer. As expected, the plot of the net helicity as a function of the *e.e.* of **BTA Cha** for various scalemic mixtures shows that chirality amplification effects govern the formation of single-handed helices (Figure 1a, black curve). Indeed, 33% *e.e.* scalemic mixtures form homochiral assemblies.[20] This demonstrates that the chirality amplification effect observed in the catalytic experiments mentioned above stems from the chirally-amplified nature of the helical scaffold of the catalyst. Based on the sign of the CD signal in the 200-270 nm region (Figure S.8),[13b] the outcome of the catalytic reaction can be correlated to the structure of the co-assemblies: scalemic mixtures biased in favour of **BTA (*R*)-Cha** form left-handed helices supporting Cu catalytic centres which in turn provide the (*S*) enantiomer of the hydrosilylation product (see a schematic representation in Scheme 1).

a)

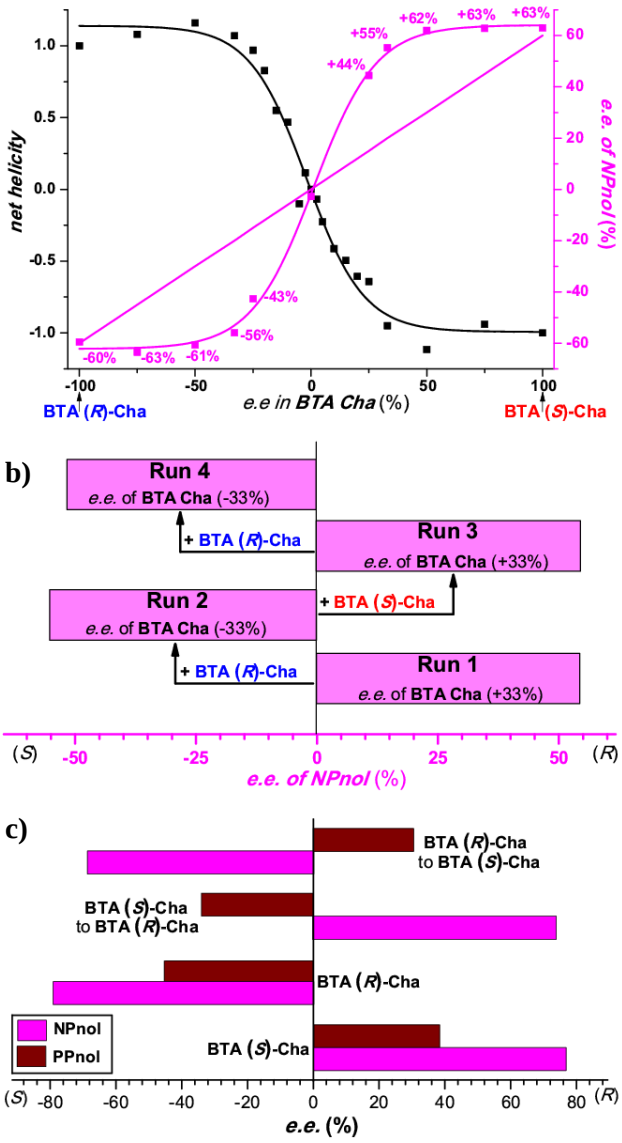

Figure 1. a) Enantiomeric excess of 1-(4-nitrophenyl)ethanol (NPnol) and net helicity versus BTA Cha enantiomeric excess. See Table S.2 for reaction conditions. The blue line represents the selectivity that would be obtained in absence of chirality amplification. The net helicity for the various co-assemblies was measured by CD spectroscopy by dividing the ellipticity (λ=305 nm) of each mixture by the ellipticity of the mixture containing enantiopure BTA Cha (Figure S.7). The curves are guides to the eye. b) Copper-catalysed hydrosilylation of NPnone with sequential additions of substrate and $PhSiH_3$. Amount of BTA Cha added during the reaction: **BTA (*R*)-Cha** (13.0 mol%, run 2), **BTA (*S*)-Cha** (26.0 mol%, run 3), **BTA (*R*)-Cha** (52.0 mol%, run 4). See Table S.3 for more experimental details. c) Copper-catalysed hydrosilylation of a 1:1 mixture of NPnone and PPnone. For the selectivity-inverting experiments, 20.0 mol% of BTA Cha was added during the reaction. See Table S.5 for more experimental details.

To demonstrate the dynamic nature of the catalytic system, we first envisaged to switch its selectivity *in situ* in a procedure involving sequential additions of NPnone and $PhSiH_3$ (Table S.3). The reaction was started with a scalemic mixture biased in favour of **BTA (*S*)-Cha** (+33% *e.e.*, run 1). After 15 minutes, complete conversion of the substrate was achieved leading to (*R*)-1-(4-nitro)phenylethanol with 53% *e.e*. Then **BTA (*R*)-Cha** was added in order to invert the enantiomer bias in the mixture (-33% *e.e.* of **BTA Cha**, run 2) and thus the handedness of the co-assemblies. The same protocol was reproduced in order to get 4 successive runs corresponding to three switches of the selectivity. The enantioselectivity for each run was deduced from the cumulative selectivity measured by chiral Gas Chromatography (GC). The full inversion of the selectivity observed for each consecutive run (Figure 1b) confirms that the enantiomeric state of the catalyst can be completely switched *in situ*. In addition, thanks to the chirally-amplified helical scaffold (*vide supra*), the selectivity of the run (54% *e.e.* on average) is close to the optimal selectivity (63% *e.e.*) achievable under these experimental conditions. In comparison, 21% *e.e.* would have been obtained in absence of chirality amplification (Figure S.10). We then measured the time required for the stereochemical switch by adding the BTA co-monomer (switch trigger) and $PhSiH_3$ (reaction trigger) at different time intervals. According to the result presented in Table S.4, full enantioinversion is achieved in *ca.* 5 seconds. The reaction time of NPnone is of the same order and thus the chirality switch cannot be fully accomplished during the conversion of this substrate. In contrast, the reaction rate of 1-(4-biphenylyl)ethanone (PPnone) is lower which allows the enantioinversion process to be performed during its transformation with no negative impact on the obtained selectivity (Scheme S.1).

The previous experiments prompted us to probe the possibility of inverting the selectivity of the catalyst during the hydrosilylation of a 1:1 mixture of NPnone and PPnone. We performed two experiments with enantiopure co-monomers (**BTA (*S*)-Cha** and **BTA (*R*)-Cha**) and two selectivity-inverting experiments starting with a scalemic mixture of enantiopure co-monomers (+60% *e.e.*→-60% *e.e.* and -60% *e.e.*→+60% *e.e.*, Table S.5). As expected, 1-(4-nitrophenyl)ethanol (NPnol) and 1-(4-biphenylyl)ethanol (PPnol) were obtained with the same preferred configuration, *i.e.* predominantly (*R*) or (*S*), when the reaction was conducted with a single enantiomer of the BTA co-monomer (Figure 1c). More precisely, the experiment performed in the presence of **BTA (*S*)-Cha** (respectively **BTA (*R*)-Cha**) provided the alcohols with optimal selectivities: +77%/+38% *e.e.* (respectively -79%/-45% *e.e.*) for NPnol and PPnol. In contrast, the alcohols were obtained with an opposite preferred configuration, *e.g.* one is predominantly (*R*) whilst the other is predominantly (*S*), when the enantiomer in excess in the co-assemblies was changed during the course of the catalytic reaction. The selectivities obtained for these experiments +74%/-34% *e.e.* or -69%/+30% *e.e.* (NPnol/PPnol) compared well with those obtained with a single co-monomer (Figure 1c). Any combination of the enantiomers is thus obtained in a one-pot procedure without significant dwindling of the catalyst selectivity.[7g,9]

We have exploited the chirality amplification properties of supramolecular polymer helices to control *in situ* the enantioselectivity displayed by phosphine copper catalytic centres located at their periphery. Switching the enantiomeric state of a catalyst in between sequential transformations could provide access to any diastereomer in cascade stereoselective reactions without purification of the reaction intermediate.[15] Also, a fast stereochemical switch is key for a precise stereocontrol of polymerization reactions.[5] The selectivity of the present catalytic system can be inverted both in between different reactions and in real time during the reaction. Improving the catalytic efficiency should be possible by combining the present concept with the recent advances achieved in tuning the composition, the structure, the stability and the stimuli-responsiveness of supramolecular polymers and assemblies.[21]

Acknowledgements

This work was supported by the French Agence Nationale de la Recherche (project ANR-13-BS07-0021 SupraCatal) and by the

China Scholarship Council (CSC, PhD grant of Y.L.). Jacques Jestin (LLB, Saclay) is acknowledged for assistance with SANS experiment and Nicolas Vanthuyne (iSm2, Marseille) for chiral HPLC analyses.

Keywords: supramolecular catalysis • selectivity-switchable catalyst • functional polymer • dynamic catalyst • chirality amplification

[1] a) N. Kumagai, M. Shibasaki, *Catal. Sci. Technol.* **2013**, *3*, 41-57; b) V. Blanco, D. A. Leigh, V. Marcos, *Chem. Soc. Rev.* **2015**, *44*, 5341-5370; c) M. Vlatković, B. S. L. Collins, B. L. Feringa, *Chem. Eur. J.* **2016**, *22*, 17080-17111.

[2] X. K. Wang, A. Thevenon, J. L. Brosmer, I. S. Yu, S. I. Khan, P. Mehrkhodavandi, P. L. Diaconescu, *J. Am. Chem. Soc.* **2014**, *136*, 11264-11267.

[3] a) A. Nojiri, N. Kumagai, M. Shibasaki, *J. Am. Chem. Soc.* **2009**, *131*, 3779-3784; b) X. Tian, C. Cassani, Y. K. Liu, A. Moran, A. Urakawa, P. Galzerano, E. Arceo, P. Melchiorre, *J. Am. Chem. Soc.* **2011**, *133*, 17934-17941.

[4] a) L. L. Lin, X. M. Feng, *Chem. Eur. J.* **2017**, *23*, 6464-6482; b) S. Krautwald, E. M. Carreira, *J. Am. Chem. Soc.* **2017**, *139*, 5627-5639.

[5] a) Coates, G. W.; Waymouth, R. M. *Science* **1995**, *267*, 217. b) C. M. Thomas, *Chem. Soc. Rev.* **2010**, *39*, 165-173.

[6] a) J. Escorihuela, M. I. Burguete, S. V. Luis, *Chem. Soc. Rev.* **2013**, *42*, 5595-5617; b) G. Romanazzi, L. Degennaro, P. Mastrorilli, R. Luisi, *ACS Catal.* **2017**, *7*, 4100-4114.

[7] a) J. B. Wang, B. L. Feringa, *Science* **2011**, *331*, 1429-1432; b) M. Vlatković, L. Bernardi, E. Otten, B. L. Feringa, *Chem. Commun.* **2014**, *50*, 7773-7775; c) C.-T. Chen, C.-C. Tsai, P.-K. Tsou, G.-T. Huang, C.-H. Yu, *Chem. Sci.* **2016**, *8*, 524-529; d) S. Mortezaei, N. R. Catarineu, J. W. Canary, *J. Am. Chem. Soc.* **2012**, *134*, 8054-8057; e) S. Mortezaei, N. R. Catarineu, X. Y. Duan, C. H. Hu, J. W. Canary, *Chem. Sci.* **2015**, *6*, 5904-5912; f) B. A. F. Le Bailly, L. Byrne, J. Clayden, *Angew. Chem. Int. Ed.* **2016**, *55*, 2132-2136; *Angew. Chem.* **2016**, *128*, 2172-2176; g) D. P. Zhao, T. M. Neubauer, B. L. Feringa, *Nat. Commun.* **2015**, *6;* h) T. Yamamoto, T. Adachi, M. Suginome, *ACS Macro Lett.* **2013**, *2*, 790–793; i) Y. Nagata, T. Nishikawa, M. Suginome, *J. Am. Chem. Soc.* **2015**, *137*, 4070–4073; j) Y. Nagata, T. Nishikawa, M. Suginome, *ACS Macro Lett.* **2016**, *5*, 519-522; k) Y.-Z. Ke, Y. Nagata, T. Yamada, M. Suginome, *Angew. Chem. Int. Ed.* **2015**, *54*, 9333–9337; *Angew. Chem.* **2015**, *127*, 9465-9469.

[8] For solvent-controlled inversion of the selectivity of an organocatalyst involved in two successive reactions see: Y. Sohtome, T. Yamaguchi, S. Tanaka, K. Nagasawa, *Org. Biomol. Chem.* **2013**, *11*, 2780-2786

[9] For a previous example of reversal of enantioselectivity during the course of an organocatalytic reaction see: S. Mortezaei, N. R. Catarineu, J. W. Canary, *Tetrahedron Lett.* **2016**, *57*, 459-462.

[10] D. Sud, T. B. Norsten, N. R. Branda, *Angew. Chem. Int. Ed.* **2005**, *44*, 2019-2021; *Angew. Chem.* **2005**, *117*, 2055-2057.

[11] a) M. Raynal, F. Portier, P. W. N. M. van Leeuwen, L. Bouteiller, *J. Am. Chem. Soc.* **2013**, *135*, 17687-17690; b) A. Desmarchelier, X. Caumes, M. Raynal, A. Vidal-Ferran, P. W. N. M. van Leeuwen, L. Bouteiller, *J. Am. Chem. Soc.* **2016**, *138*, 4908-4916.

[12] a) A. R. A. Palmans, E. W. Meijer, *Angew. Chem. Int. Ed.* **2007**, *46*, 8948-8968; b) E. Yashima, N. Ousaka, D. Taura, K. Shimomura, T. Ikai, K. Maeda, *Chem. Rev.* **2016**, *116*, 13752-13990. c) J. Jiang, G. Ouyang, L. Zhang, M. Liu, *Chem. Eur. J.* **2017**, 23, 9439.

[13] a) S. Cantekin, T. F. A. de Greef, A. R. A. Palmans, *Chem. Soc. Rev.* **2012**, *41*, 6125-6137; b) Y. According to the assignment made by Meijer and co-workers: M. M. J. Smulders, T. Buffeteau, D. Cavagnat, M. Wolffs, A. P. H. J. Schenning, E. W. Meijer, *Chirality* **2008**, *20*, 1016-1022.

[14] A. J. Jordan, G. Lalic, J. P. Sadighi, *Chem. Rev.* **2016**, *116*, 8318-8372.

[15] S.-L. Shi, Z. L. Wong, S. L. Buchwald, *Nature* **2016**, *532*, 353-356.

[16] M. M. J. Smulders, I. A. W. Filot, J. M. A. Leenders, P. Van der Schoot, A. R. A. Palmans, A. P. H. J. Schenning, E. W. Meijer, *J. Am. Chem. Soc.* **2010**, *132*, 611-619.

[17] a) A. Desmarchelier, M. Raynal, P. Brocorens, N. Vanthuyne, L. Bouteiller, *Chem. Commun.* **2015**, *51*, 7397-7400; b) X. Caumes, A. Baldi, G. Gontard, P. Brocorens, R. Lazzaroni, N. Vanthuyne, C. Troufflard, M. Raynal, L. Bouteiller, *Chem. Commun.* **2016**, *52*, 13369-13372; c) A. Desmarchelier *et al. Soft Matter* **2016**, *12*, 7824-7838.

[18] The CD experiments were conducted in methylcyclohexane ([**BTA Cha**)/[**BTA**$^{\mathbf{PPh2}}$]=2.2, 2.0 mM).

[19] S. Allenmark, *Chirality* **2003**, *15*, 409-422.

[20] The same result is obtained when the CD spectra are processed in order to remove the contribution of the dimers to the overall CD signal (Figures S.8 and S.9). .

[21] a) J. Kang, D. Miyajima, T. Mori, Y. Inoue, Y. Itoh, T. Aida, *Science* **2015**, *347*, 646-651; b) P. Besenius, *J. Polym. Sci. Pol. Chem.* **2017**, *55*, 34-78; c) J. R. Nitschke, *Nature* **2009**, *462*, 736-738; d) R. A. R. Hunt, S. Otto, *Chem. Commun.* **2011**, *47*, 847-858.

Change it easy! A first step towards selecting the configuration of consecutively formed stereogenic centres in cascade or polymerization reactions has now been achieved by controlling the enantioselectivity of a metal catalyst in real time. The strategy relies on the complete and fast stereochemical switch of the handedness of the dynamic helices supporting the catalytic centres.

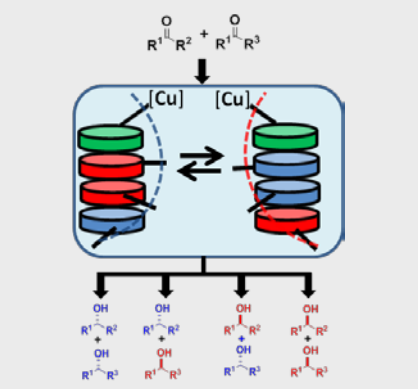

Dr. Jeremy M. Zimbron, Dr. Xavier Caumes, Yan Li, Dr. Christophe M. Thomas, Dr. Matthieu Raynal, Dr. Laurent Bouteiller*

Real-time control of the enantioselectivity of a supramolecular catalyst allows selecting the configuration of consecutively formed stereogenic centres

Supporting Information

Supplementary Tables. Catalytic experiments: chirality induction and amplification [Tables S.1 and S.2]

Table S.1 Repeatability of the catalytic experiments for the hydrosilylation of 1-(4-nitrophenyl)ethanone.[a]

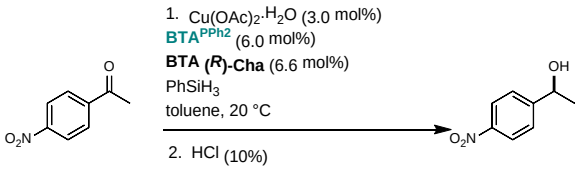

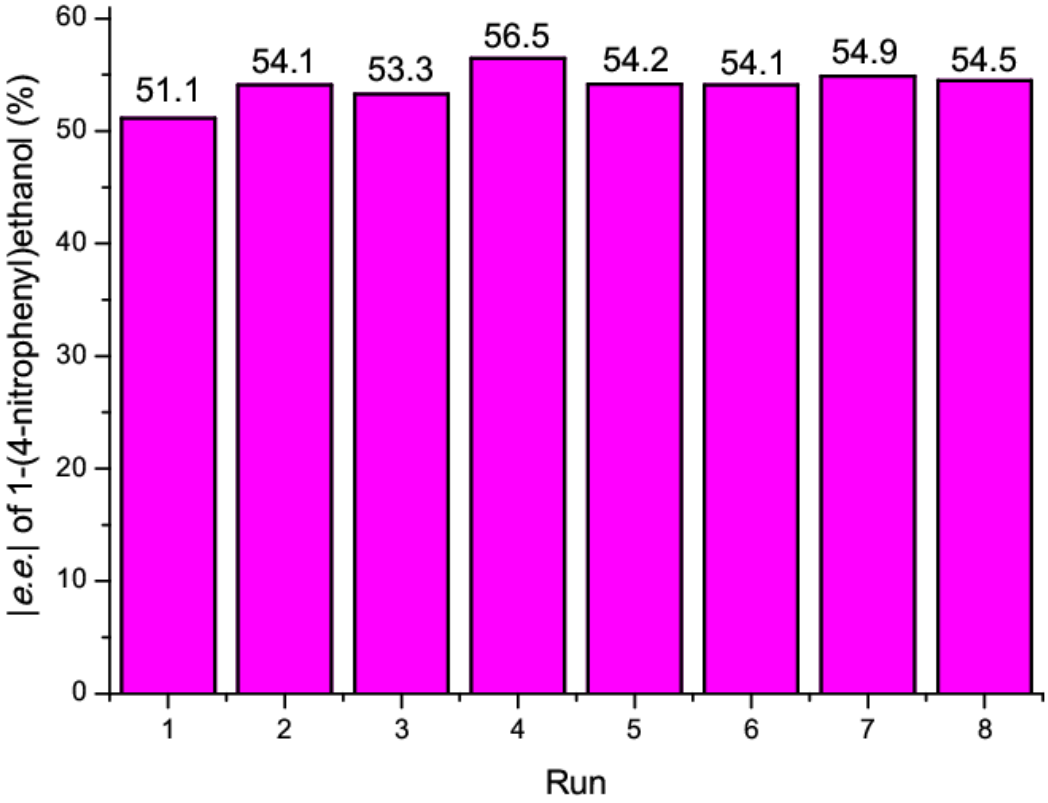

[a] The above table summarizes 8 batches of reactions that have been repeated in the same conditions namely: 1-(4-nitrophenyl)ethanone (0.29 M), $Cu(OAc)_2 \cdot H_2O$ (3.0 mol%), **BTA^{PPh2}** (6.0 mol%, 16.9 mM), **BTA (*R*)-Cha** (6.6 mol%, 18.6 mM), $PhSiH_3$ (0.29 M), toluene, 20°C, 30 min. Conversion >99% was obtained for all runs as determined by GC and ^{1}H NMR analyses. Based on this repeatability assessment, a mean *e.e.* value of 54.1% is determined over the 8 runs. The standard deviation is s=1.4 and the variance is s^2=2.0. Accordingly, an error bar of ± ½ variance (±1% *e.e.*) was set to the *e.e.* values obtained with mixtures of **BTA^{PPh2}** and **BTA (*R*)-Cha** (Table 1).

Table S.2 Hydrosilylation of 1-(4-nitrophenyl)ethanone with a scalemic mixture of enantiopure **BTA Cha** co-monomers (25% *e.e.*).[a]

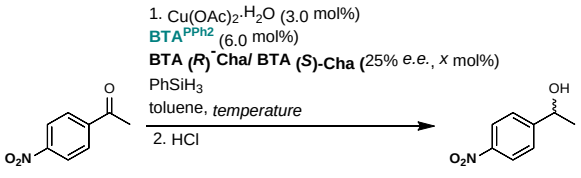

Entry	T (°C)	**BTA (*R*)-Cha** (mol%)	**BTA (*S*)-Cha** (mol%)	expected unamplified *e.e.* (%)[b]	obtained *e.e.* (%)	R_{ampl}[c]
1	**20**	6.6	0	-	-54	-
2	**20**	4.1	2.5	-13.5	-39	2.86
3	**20**	13.2	0	-	-54	-
4	**20**	8.2	5.0	-13.5	-45	3.33
5	**0**	6.6	0	-	-63	-
6	**0**	4.1	2.5	-15.8	-27	1.72
7	**0**	13.2	0	-	-63	-
8	**0**	8.2	5.0	-15.8	-45	2.87
9	**-25**	6.6	0	-	-78	-
10	**-25**	4.1	2.5	-19.5	-29	1.47
11	**-25**	13.2	0	-	-78	-
12	**-25**	8.2	5.0	-19.5	-34	1.72

[a] Reaction conditions: 1-(4-nitrophenyl)ethanone (0.29 M), $Cu(OAc)_2 \cdot H_2O$ (3.0 mol%), **BTA^{PPh2}** (6.0 mol%, 16.9 mM), 25% *e.e.* scalemic mixture biased in favour of **BTA (*R*)-Cha** (x mol%), $PhSiH_3$ (0.29 M), toluene. Conversion >99% was obtained for all entries as determined by GC and ^{1}H NMR analyses.

[b] Expected *e.e.* in the absence of any chirality amplification effect, considering the optical purity of the engaged scalemic mixture of enantiopure **BTA Cha**.

[c] Majority-rule factor defined as R_{ampl}= (obtained *e.e.*)/(expected *e.e.* in absence of chirality amplification). R_{ampl}=1.0 means no chirality amplification and the higher R_{ampl} the higher the chirality amplification effect.

Conditions highlighted in orange have been selected for probing the chirality amplification effect displayed by the catalytic assemblies (Fig. 1a). Reaction conditions: 1-(4-nitrophenyl)ethanone (0.29 M), $Cu(OAc)_2 \cdot H_2O$ (3.0 mol%), **BTA^{PPh2}** (6.0 mol%, 16.9 mM), **BTA (*R*)-Cha**/**BTA (*S*)-Cha** (x % e.e., 13.2 mol%), $PhSiH_3$ (0.29 M), toluene, 0°C. Conversion >99% was obtained in all cases as determined by GC and ^{1}H NMR analyses.

Supplementary Tables and Figures: Characterization of the Cu supramolecular catalyst by means of various spectroscopic and scattering analyses [Figures S.1 to S.9]

Postulated active copper hydride species (made by reacting **BTA^{PPh2}**, $Cu(OAc)_2 \cdot H_2O$ and $PhSiH_3$) are poorly stable under our experimental conditions in the absence of substrate or product. Accordingly, in the following, we will focus on the characterization of the co-assemblies formed by mixing: i) **BTA^{PPh2}** and **BTA (*R*)-Cha**, and ii) **BTA^{PPh2}** coordinated to Cu (**BTA^{PPh2}**/$Cu(OAc)_2 \cdot H_2O$= 2.0) and **BTA (*R*)-Cha**.

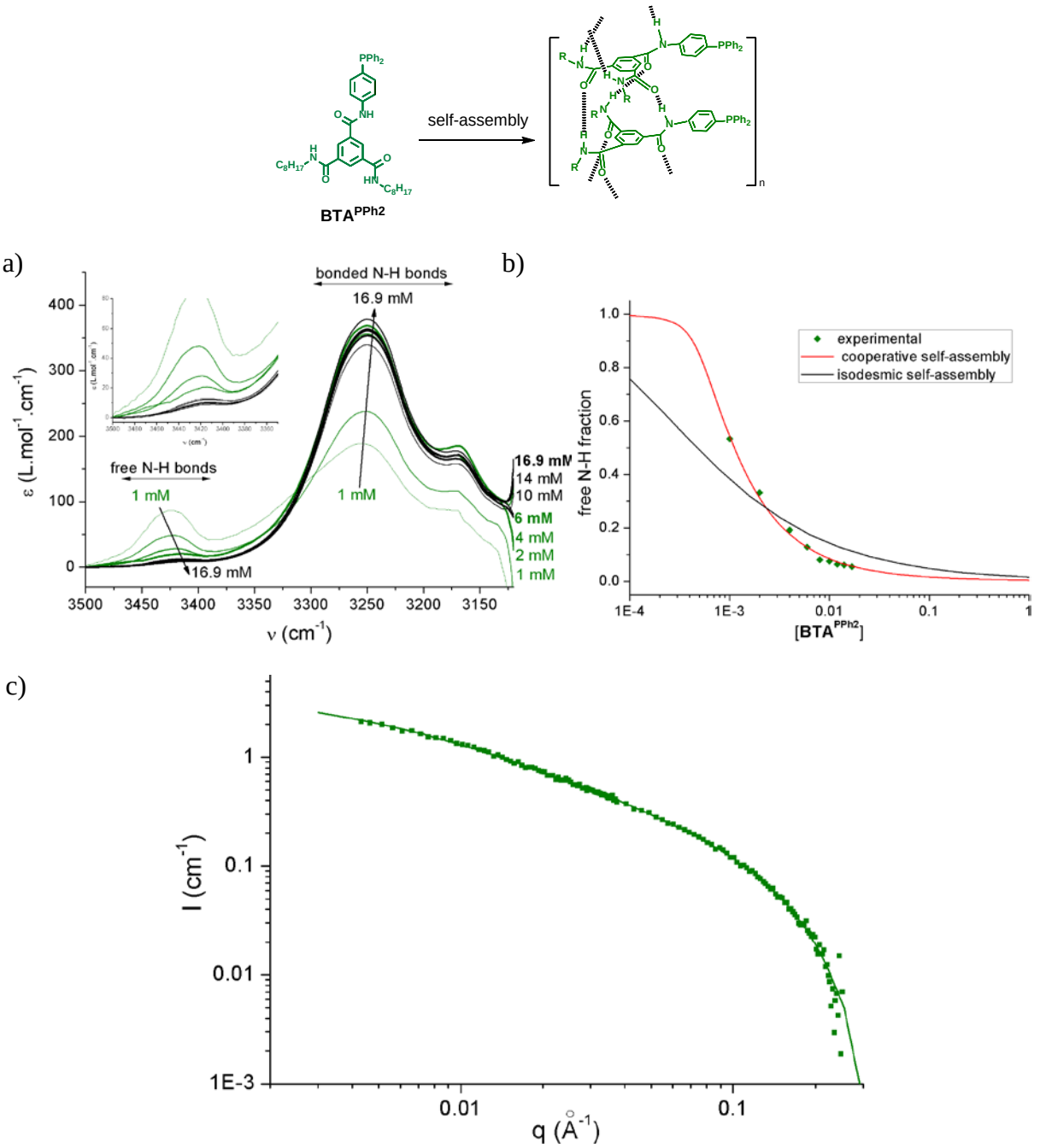

Figure S.1 Characterization of the homo-assemblies formed by **BTA^{PPh2}**. (a) FT-IR analyses of **BTA^{PPh2}** at various concentrations in toluene (20 °C). Zoom on the N-H region. (b) Plot of the free N-H fraction as a function of the concentration in **BTA^{PPh2}**. (c) SANS analysis of **BTA^{PPh2}** (11.7 g.dm^{-3}, 16.9 mM) in toluene-d_8 (20°C).

The absorption band at ν=3235 cm^{-1} (a) is diagnostic of the bonded N-H present in stacks whilst the absorption band at ν=3430 cm^{-1} is diagnostic of free N-H (belonging either to monomers or to BTA molecules located at the chain-ends of the assemblies). The fraction of free N-H can be deduced from these FT-IR data by a linear regression of the plot of ([**BTA^{PPh2}**]×l)/A_b^{N-H} versus A_f^{N-H}/A_b^{N-H} with [**BTA^{PPh2}**] = total concentration in **BTA^{PPh2}**, l = cell pathlength, A_b^{N-H} = maximum of the absorption band for bonded N-H, A_f^{N-H} = maximum of the absorption band for free N-H. It provides the following value for the molar extinction coefficients: ε_b^{N-H}=390 L.mol^{-1}.cm^{-1} and ε_f^{N-H}=158 L.mol^{-1}.cm^{-1}. The data in (b) can be perfectly fitted by a cooperative model for self-assembly[1] (K_2/K model) but not by an isodesmic model.[2] The fit gives the following values: K_2=35 M^{-1}, K=1794 M^{-1}, K/K_2=51 (DPn=18 and DPw=75 for [BTA^{PPh2}]=16.9 mM). SANS analysis of **BTA^{PPh2}** (c) is fitted with the form factor for long and rigid rods with a circular cross-section and a uniform scattering length density (with the DANSE software SasView). The fit yields a radius of 11.5 Å and a length of 204 Å for the stacks formed by **BTA^{PPh2}**.

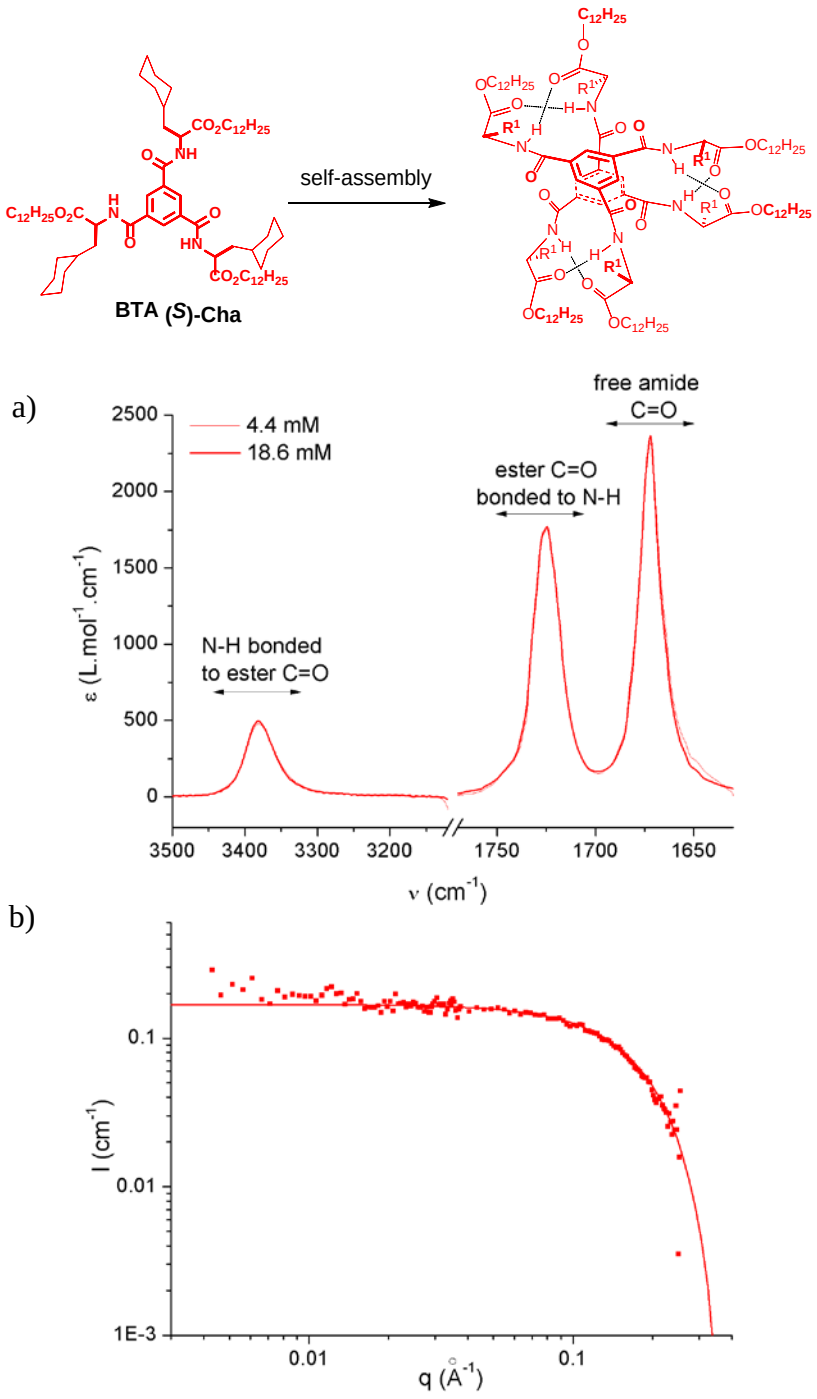

Figure S.2 Characterization of the homo-assemblies formed by **BTA (*S*)-Cha**. (a) FT-IR analyses of **BTA Cha** at 4.4 mM and 18.6 mM in toluene (20 °C). Zoom on the N-H and C=O region. (b) SANS analysis of **BTA (*S*)-Cha** (21.9 g.dm^{-3}, 18.6 mM) in toluene-d_8 (20°C).

The absorption band at ν=3381 cm^{-1} (a) corresponds to N-H bonded to carbonyl ester functions and is diagnostic of the hydrogen-bonded network present in the ester-bonded dimers formed by ester BTAs. SANS analysis of **BTA (*S*)-Cha** (b) confirms the formation of small assemblies since the scattering curve can be fitted according to a form factor for spherical objects having 1.5 times the molar mass of the monomer (result of the fit: r = 12.0 Å and M = 1750 g.mol^{-1}). More details on the structure and stability of the ester-bonded dimers formed by ester BTAs can be found in the literature.[3]

Characterization of the co-assemblies formed by BTA^{PPh2}, coordinated or not to copper, and BTA (*S*)-Cha.

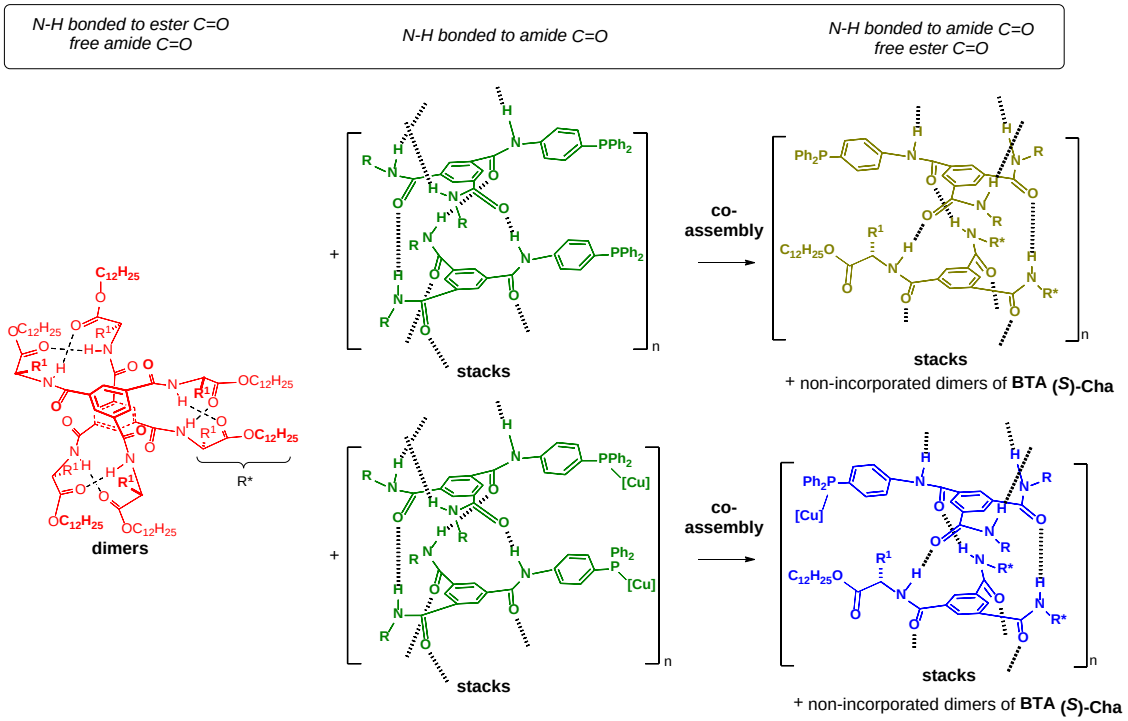

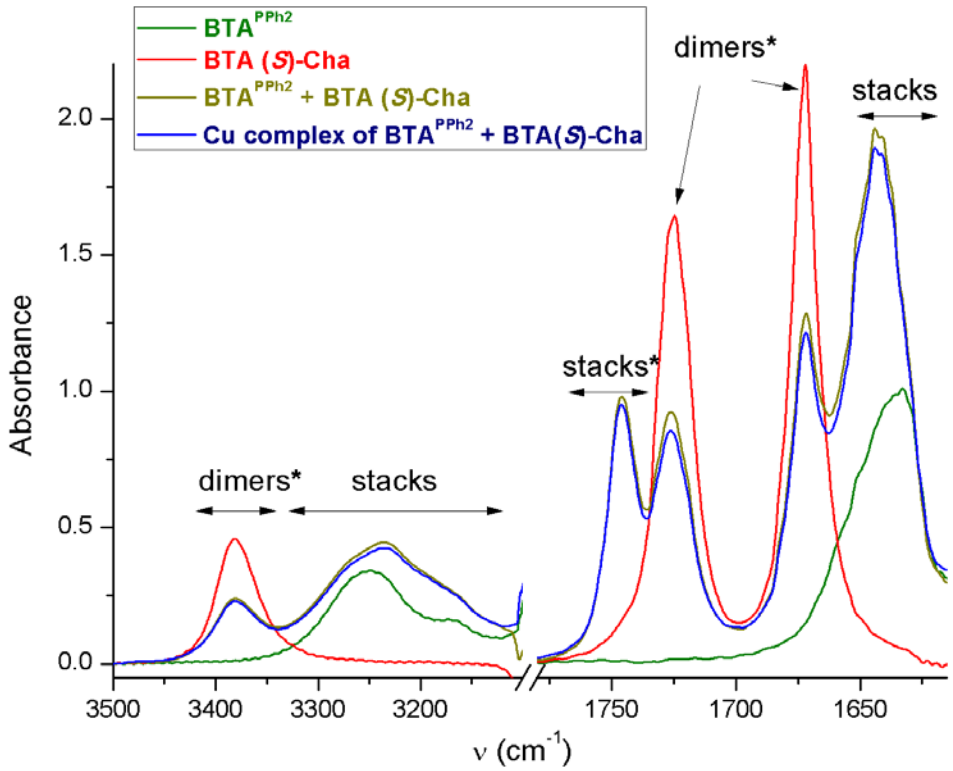

Figure S.3 FT-IR analyses of **BTA^{PPh2}** (16.9 mM), of **BTA (*S*)-Cha** (18.6 mM) and of the mixtures of **BTA^{PPh2}** (16.9 mM) and **BTA (*S*)-Cha** (18.6 mM) with and without Cu coordinated to **BTA^{PPh2}** in toluene at 20 °C.

***** These absorption bands belong exclusively to **BTA (*S*)-Cha** either in dimers or in stacks (co-assembly).

Upon co-assembly, a fraction of **BTA (*S*)-Cha** molecules is incorporated into the stacks formed by **BTA^{PPh2}** as indicated by: i) the decreased intensity of the absorption bands belonging to **BTA (*S*)-Cha** (ν_{N-H}=3380 cm^{-1}, $\nu_{esterC=O}$=1725 cm^{-1} and $\nu_{amideC=O}$=1672 cm^{-1}), ii) the increased intensity of the absorption bands corresponding to stacks (ν_{N-H}=3235 cm^{-1} and $\nu_{amideC=O}$=1645 cm^{-1}) and iii) the emergence of a new absorption band at ν=1745 cm^{-1} which corresponds to free ester C=O functions and thus belongs exclusively to **BTA (*S*)-Cha** molecules incorporated into stacks. The FT-IR spectra of the mixtures with and without Cu coordinated to **BTA^{PPh2}** are virtually identical indicating that the presence of the Cu has little influence on the composition of the co-assemblies. For the determination of the amount of **BTA (*S*)-Cha** incorporated into stacks, see below.

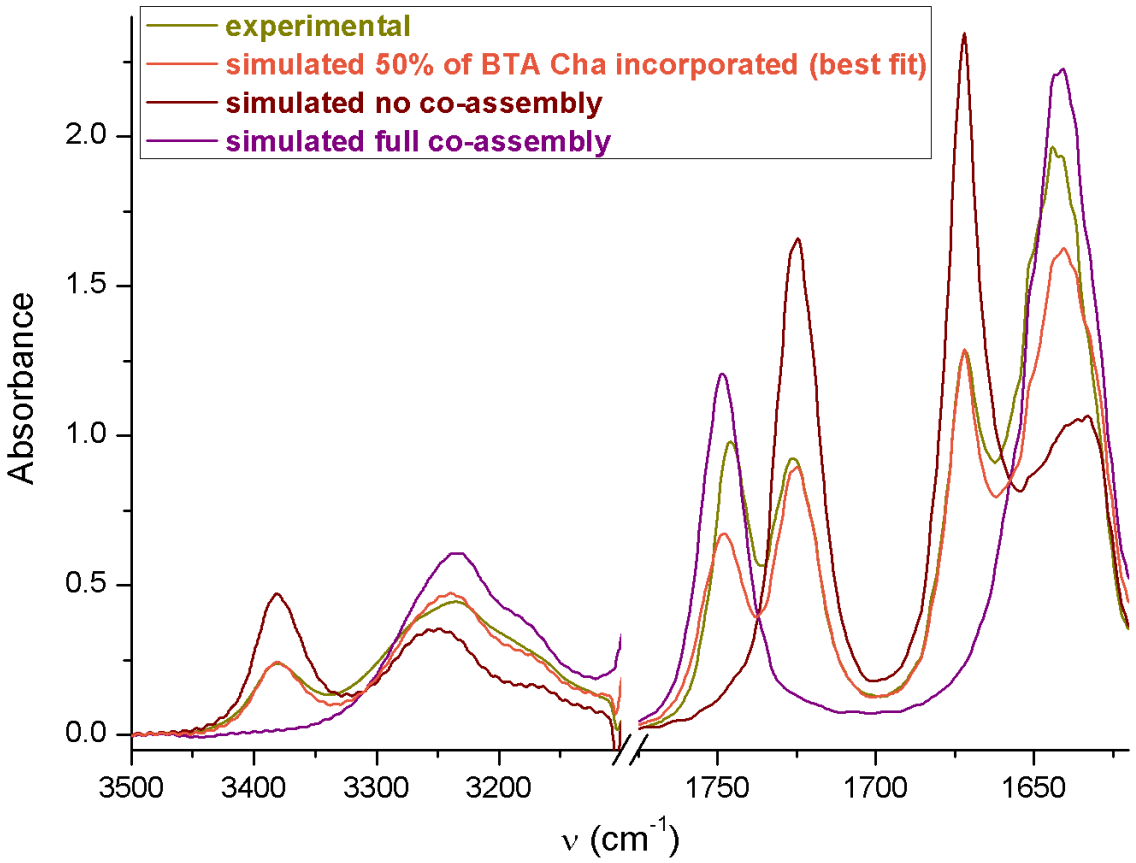

Figure S.4 Quantification of the amount of **BTA (*S*)-Cha** present in the co-assemblies.[4] FT-IR analysis of the mixture of **BTA^{PPh2}** (16.9 mM) and **BTA (*S*)-Cha** (18.6 mM) in toluene at 20°C. Simulated spectra for the extreme cases for which all or no **BTA (*S*)-Cha** is present in the co-assemblies. The fraction of **BTA (*S*)-Cha** incorporated into stacks (relatively to the amount of **BTA (*S*)-Cha** introduced initially, *i.e.* 18.6 mM) is 50% as deduced from the best fit with the simulated FT-IR spectra (estimated error 10%). It means that ~35% of the BTA co-monomers present in the co-assemblies are **BTA Cha**.

* The simulated spectrum of the stacks for the co-assemblies is the weighted average of the contribution of each monomer (**BTA^{PPh2}** and **BTA (*S*)-Cha**) present in the stacks. The spectroscopic signature of **BTA (*S*)-Met**,[3a, 3b] an ester BTA which forms stacks in solution contrarily to **BTA (*S*)-Cha**, was selected for the spectrum representing **BTA (*S*)-Cha** in the co-assemblies. The quality of the fit validates the hypothesis that the conformation of **BTA (*S*)-Cha** molecules in the co-assembly is similar to that of **BTA (*S*)-Met** molecules in the stacks.

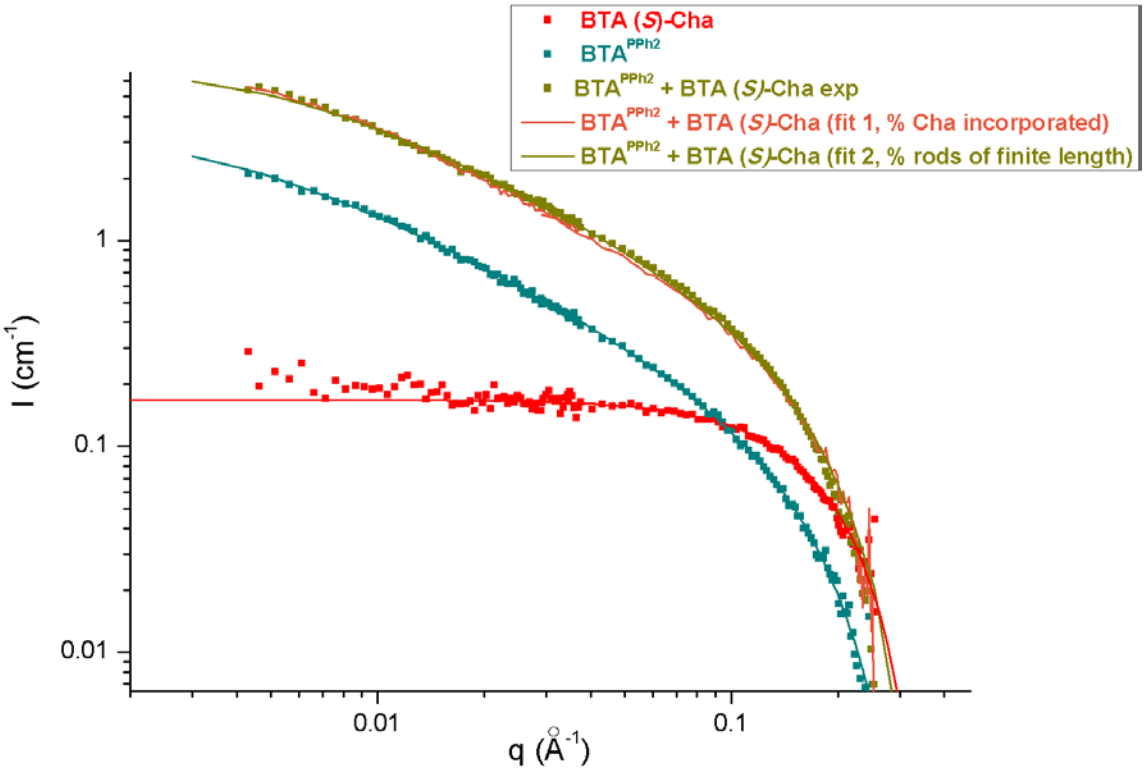

Figure S.5 Characterization by SANS analyses of the composition of the co-assemblies formed between **BTA^{PPh2}** (11.7 g.dm^{-3}, 16.9 mM) and **BTA (*S*)-Cha** (21.9 g.dm^{-3}, 18.6 mM) in toluene-d_8 (20°C).

Fit 1: the experimental curve for the mixture of **BTA^{PPh2}** and **BTA (*R*)-Cha** is fitted according to the hypothesis that **BTA (*R*)-Cha** in part co-assembles with **BTA^{PPh2}** and that the remaining **BTA (*R*)-Cha** exists as dimers. The hypothesis is confirmed by the quality of the fit and by FT-IR analyses presented above (Figure S.4). The fit gives the following results: 67% of **BTA (*R*)-Cha** is incorporated into stacks. This value is in agreement with that deduced from FT-IR analysis (50 %, see Figure S.4).

Fit 2: the length of the co-assemblies formed by **BTA^{PPh2}** and **BTA (*R*)-Cha** is determined by fitting the SANS analysis with a form factor for rigid rods of finite length with a circular cross-section and a uniform scattering length density. It gives a length of 145 Å for the co-assemblies which are hence shorter than the stacks formed by **BTA^{PPh2}** (204 Å).

For the results of the fits corresponding to SANS analyses of **BTA^{PPh2}** and **BTA (*R*)-Cha**, see Figures S.1 and S.2 respectively.

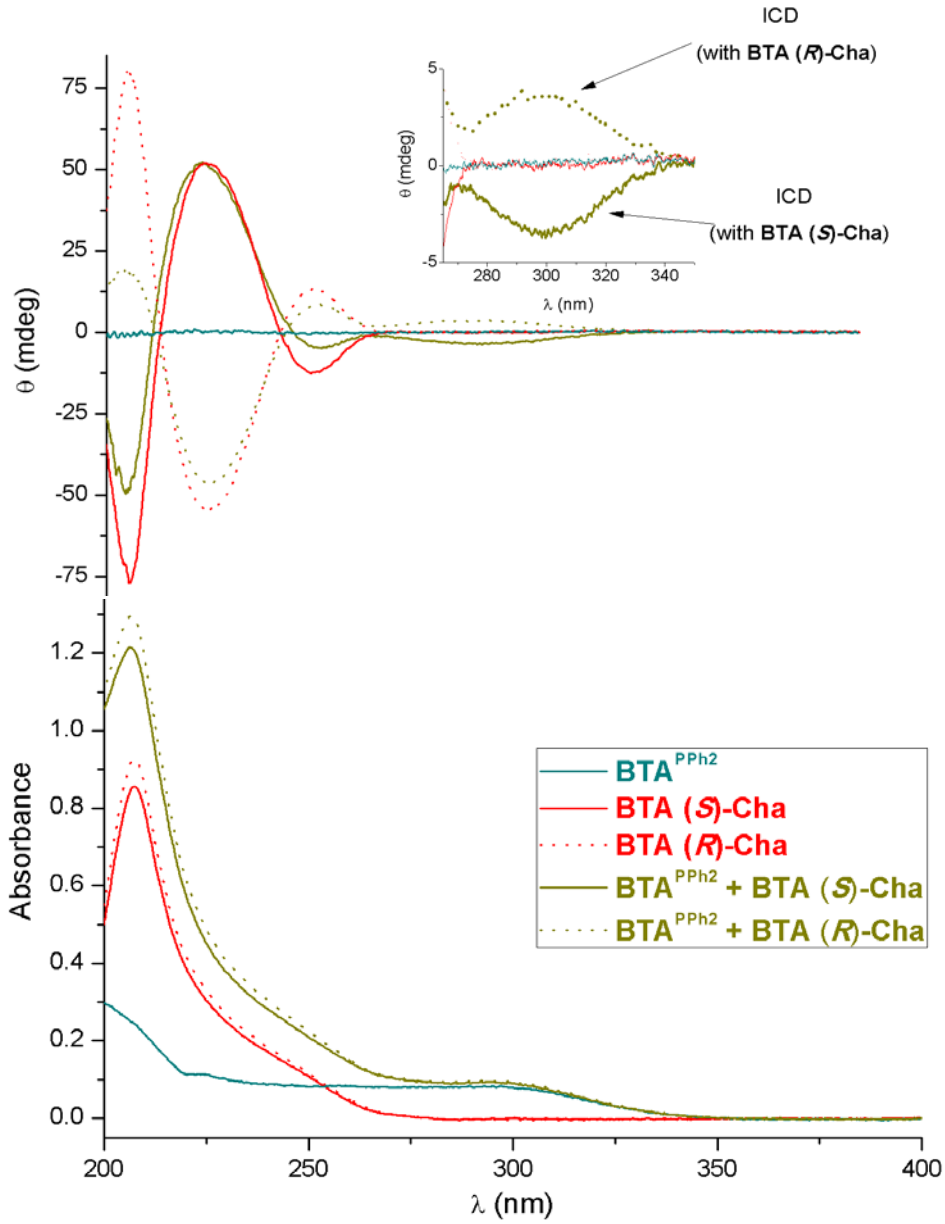

Figure S.6 CD (top) and UV (bottom) analyses of **BTA^{PPh2}** (0.625 mM), of **BTA (*S*)-Cha** (1.375 mM), of **BTA (*R*)-Cha** (1.375 mM) and of the mixtures of **BTA^{PPh2}** (0.625 mM) and **BTA (*S*)-Cha** (1.375 mM) and of **BTA^{PPh2}** (0.625 mM) and **BTA (*R*)-Cha** (1.375 mM) in methylcyclohexane at 20 °C.

CD analyses of **BTA (*S*)-Cha** and **BTA (*R*)-Cha** with three maxima in the region of 200-270 nm are diagnostic of the ester-bonded dimers.[3] Mixtures of **BTA^{PPh2}** and **BTA Cha** show, in addition to CD signals in the 200-270 nm region, a Cotton effect centered at λ=310 nm, of same intensity but opposite sign depending on the enantiomer of **BTA Cha** present in the mixture. As only **BTA^{PPh2}** absorbs in this region, this signal is called an induced CD signal (ICD)[5] and thus indicates that the achiral ligand is located in the chiral environment formed by the helical BTA co-assemblies. Also, enantiomers of **BTA Cha** are able to fully switch the chirality induced to **BTA^{PPh2}**.

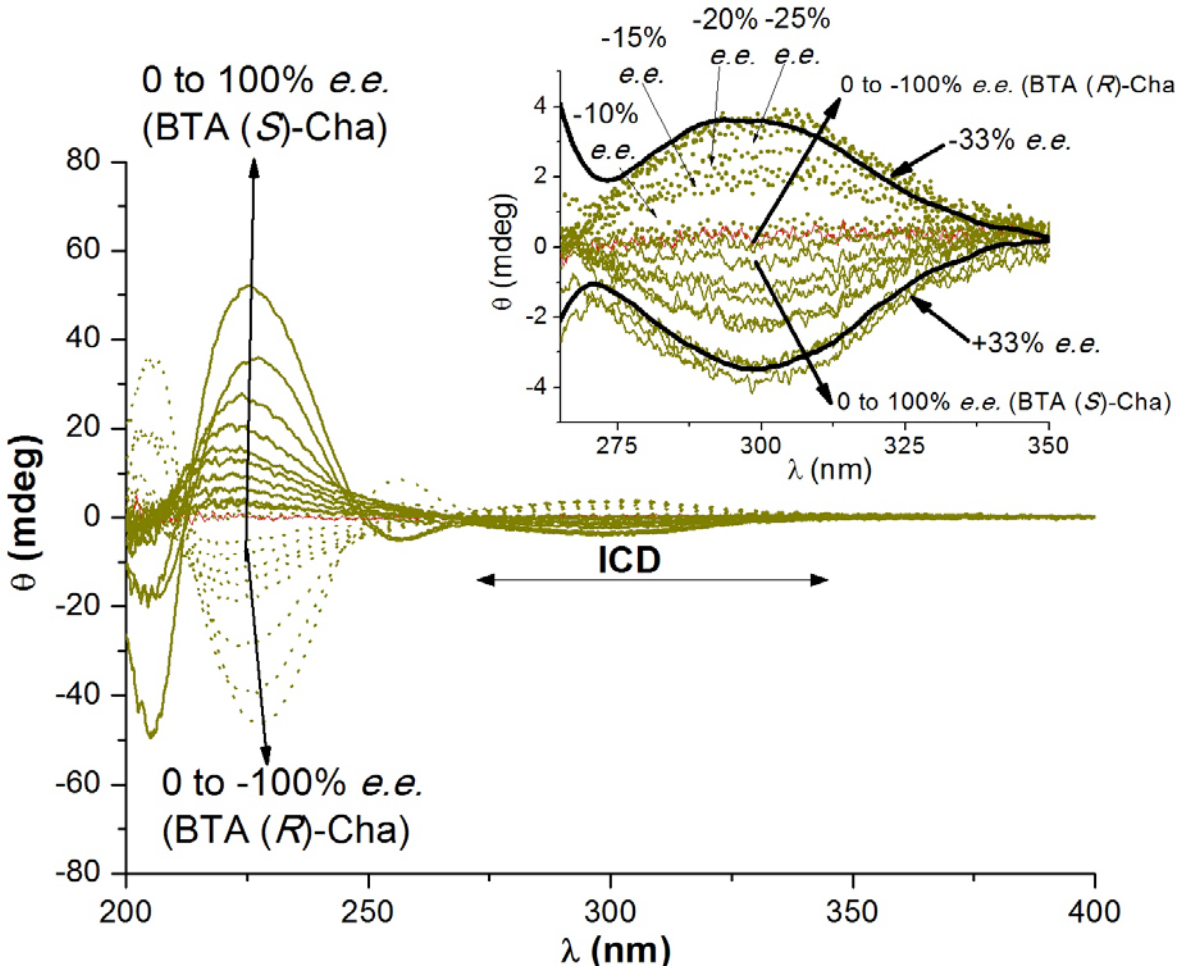

Figure S.7 CD analyses of mixtures of **BTA^{PPh2}** (0.625 mM) and **BTA Cha** of various enantiomeric excesses (1.375 mM) in methylcyclohexane at 20°C. Inset: zoom on the ICD signals.

The mixtures with +33% *e.e.* and -33% *e.e.* have been thickened since a maximum intensity of the ICD signal is reached for these mixtures. CD analyses were recorded for the following $|e.e.|$ in **BTA Cha**: 0%, 2.5%, 5%, 10%, 15%, 20%, 25%, 33%, 50%, 75% and 100%.

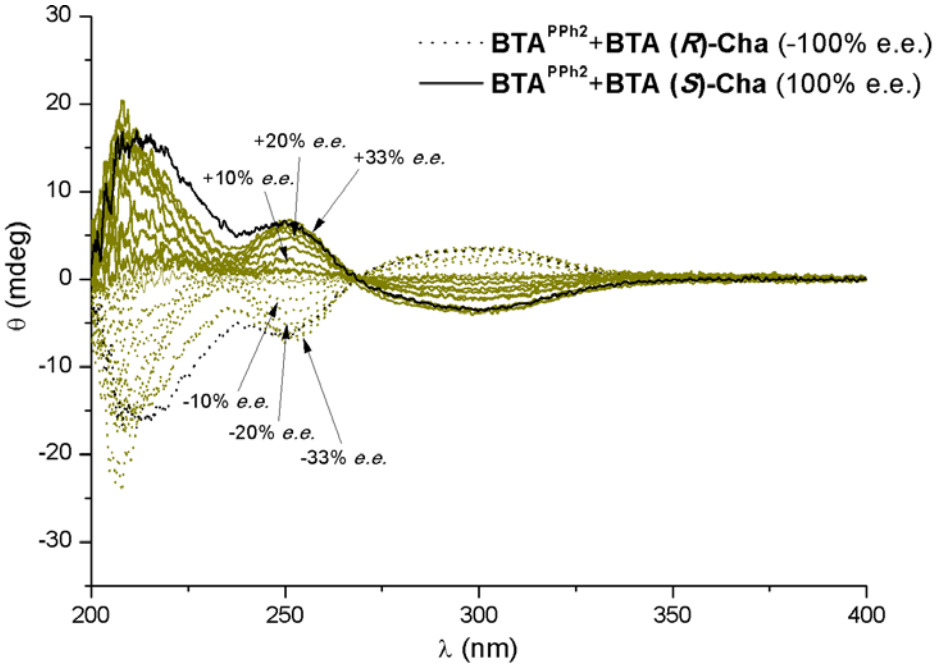

Figure S.8 "Diluted majority rule experiments" of Fig. S.7 processed in order to remove the contribution of **BTA Cha** dimers to the overall CD signal. The amount of **BTA Cha** that remains as dimers in the mixtures (conditions indicated in Fig. S.7) has been quantified to 80% by means of FT-IR analyses (data not shown).

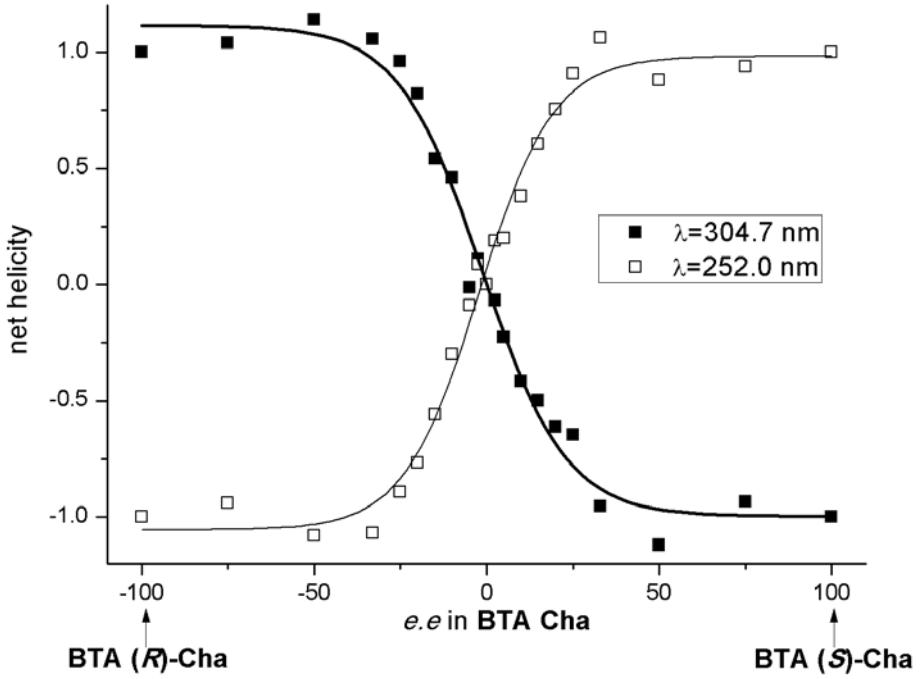

Figure S.9 "Diluted majority rule experiments": Net helicity as a function of the enantiomeric excess of **BTA Cha** determined according to CD analyses shown in Figures S.8. The net helicities were obtained by dividing the ellipticities at λ=305 nm and λ=252 nm for each mixture by the ellipticities measured for the mixture containing enantiopure **BTA Cha**. The lines are drawn as a guide to the eye.

Supplementary Tables, Schemes and Figures: selectivity-switching experiments [Tables S.3 to S.5, Scheme S.1, Figure S.10]

Table S.3 Copper-catalysed hydrosilylation of 1-(4-nitrophenyl)ethanone with successive additions of substrate and $PhSiH_3$.[a],[b],[c]

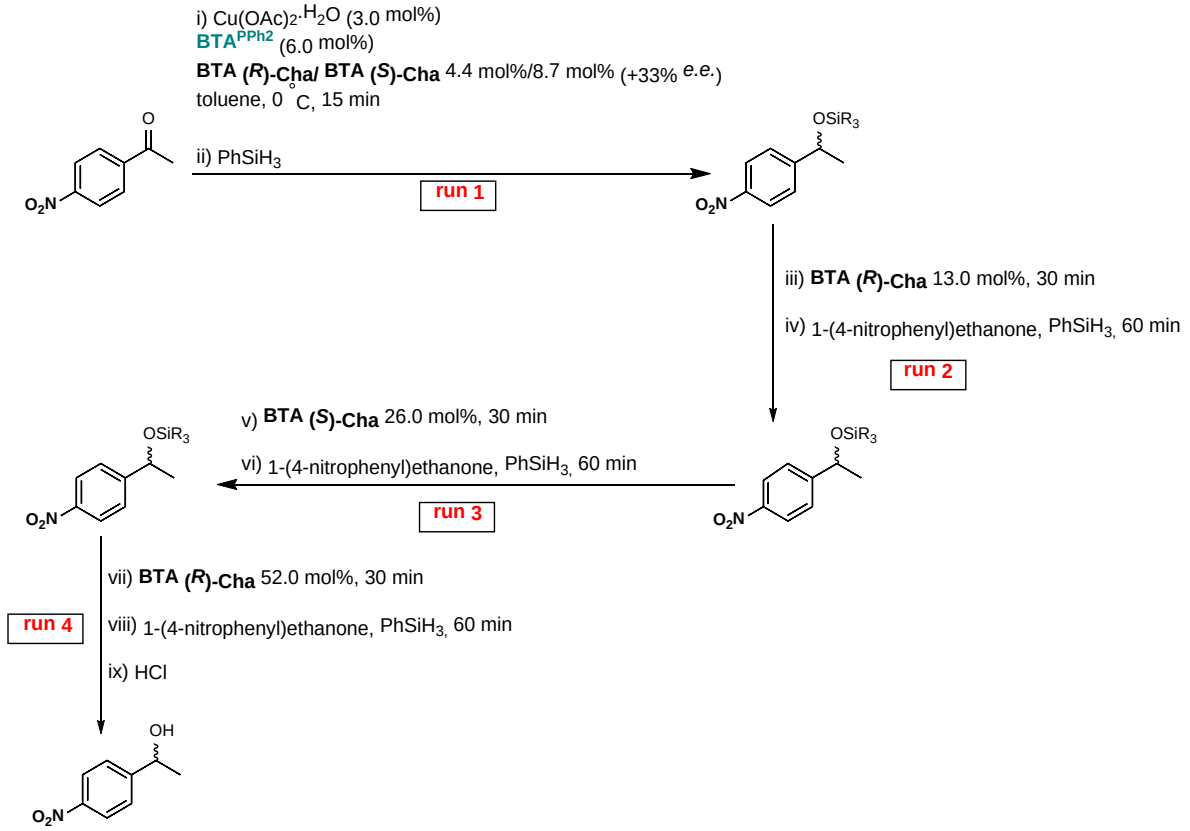

Run	**BTA (*R*)-Cha** (mol%)	**BTA (*S*)-Cha** (mol%)	obtained *e.e.* (%)	*e.e.* for the run *(%)*
1	4.4	8.7	+53 (*R*)	+53 (*R*)
2	17.4	8.7	-2 (*S*)	-56 (*S*)
3	17.4	34.7	+17 (*R*)	+53 (*R*)
4	69.4	34.7	0	-52 (*S*)

[a] Reaction conditions: 1-(4-nitrophenyl)ethanone (4×100 mol% = 400 mol% in total), $Cu(OAc)_2 \cdot H_2O$ (3.0 mol%), **BTA^{PPh2}** (6.0 mol%), **BTA (*R*)-Cha**/**BTA (*S*)-Cha** (|***e.e.***| = **33** %), $PhSiH_3$ (200 mol% for run 1and then 100 mol% for run 2, run 3 and run 4 = 500 mol% in total), toluene, 0 °C. For the exact amount of BTA Cha present in each run, see the table. Conversion >99% was obtained for all runs as determined by GC and ^1H NMR analyses. For the GC analyses corresponding to each run see pages S.23 and S.24..

[b] The optimal selectivity for the supramolecular Cu catalyst under these conditions as determined in Fig. 1a is 63% *e.e.* This is the selectivity expected for a catalyst with a fully chirally-amplified helical backbone. In contrast, 21% *e.e.* (0.33 × 63) would be obtained in absence of chirality amplification.

[c] The reaction times for the conversion of the substrate and for the stereochemical switch were not optimized (see Table S.4).

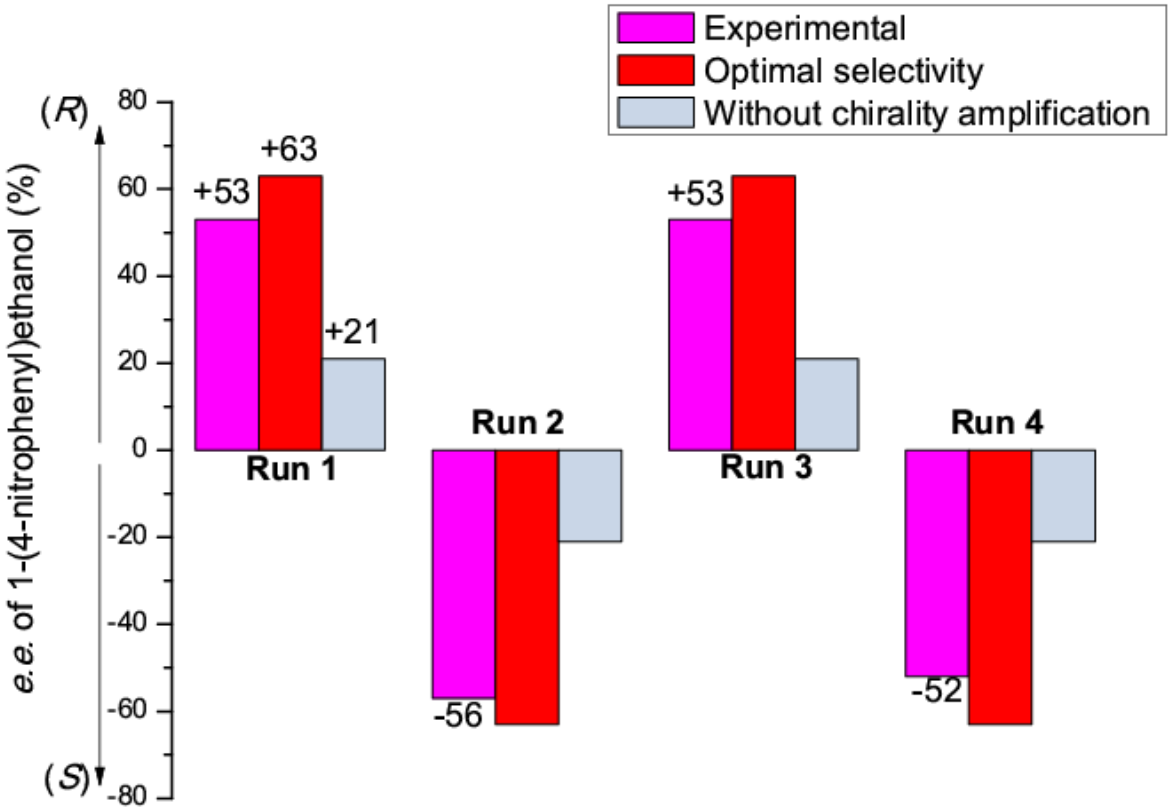

Figure S.10 Copper-catalysed hydrosilylation of 1-(4-nitrophenyl)ethanone with successive additions of substrate and $PhSiH_3$. Comparison of the enantioselectivity of the runs, the optimal selectivity and the selectivity in absence of chirality amplification.

For the conditions and results of the sequential reaction and the definitions of the optimal selectivity and of the selectivity in absence of chirality amplification see the Table S.3.

Table S.4 Determination of the time required for switching the selectivity for the copper-catalysed hydrosilylation of 1-(4-nitrophenyl)ethanone.[a]

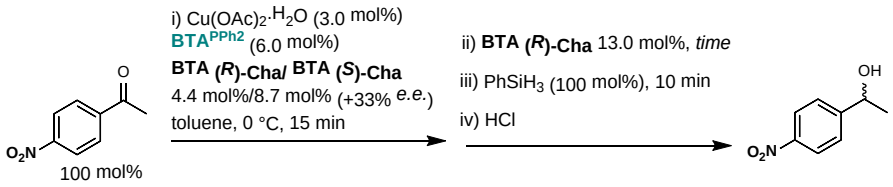

Entry	Time (s)	*e.e. (%)*
0	no **BTA (*R*)-Cha** addition	+60 (*R*)
1	0	+17 (*R*)[b]
2	5	-56 (*S*)
3	20	-60 (*S*)
4	60	-62 (*S*)

[a] Reaction conditions: 1-(4-nitrophenyl)ethanone (100 mol%), $Cu(OAc)_2 \cdot H_2O$ (3.0 mol%), **BTA^{PPh2}** (6.0 mol%), **BTA (*R*)-Cha**/**BTA (*S*)-Cha** (4.4 mol%/8.7 mol%, +33% *e.e.*), toluene, 0 °C. **BTA (*R*)-Cha** (13.0 mol%) was added and then $PhSiH_3$ (100 mol%) after a given time. Conversion >99% was obtained for all entries as determined by GC and ^1H NMR analyses. For the GC analyses corresponding to a time of 5 seconds (entry 2) see page S.35.

[b] **BTA (*R*)-Cha** and $PhSiH_3$ were mixed together and added together to the precatalytic mixture. In these conditions, the selectivity switch was not complete. It means that the conversion of 1-(4-nitrophenyl)ethanone and the stereochemical switch occur at the same timescale.

Scheme S.1 Stereochemical switch during the conversion of 1-(4-biphenylyl)ethanone.[a]

a)

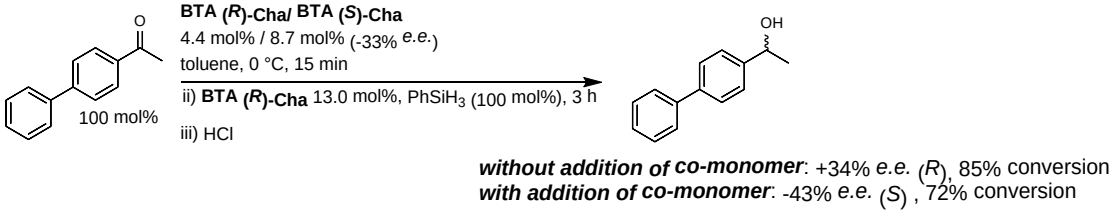

Reaction conditions: 1-(4-biphenylyl)ethanone (100 mol%), $Cu(OAc)_2 \cdot H_2O$ (3.0 mol%), **BTA^{PPh2}** (6.0 mol%), **BTA (*R*)-Cha/BTA (*S*)-Cha** (4.4 mol%/8.7 mol%, +33% *e.e.*), toluene, 0 °C. **BTA (*R*)-Cha** (13.0 mol%) and $PhSiH_3$ (100 mol%) were mixed and added at the same time. The conversion was determined by GC and ^1H NMR analyses. For the chiral HPLC analyses with and without switch, see pages S.26 and S.27.

b)

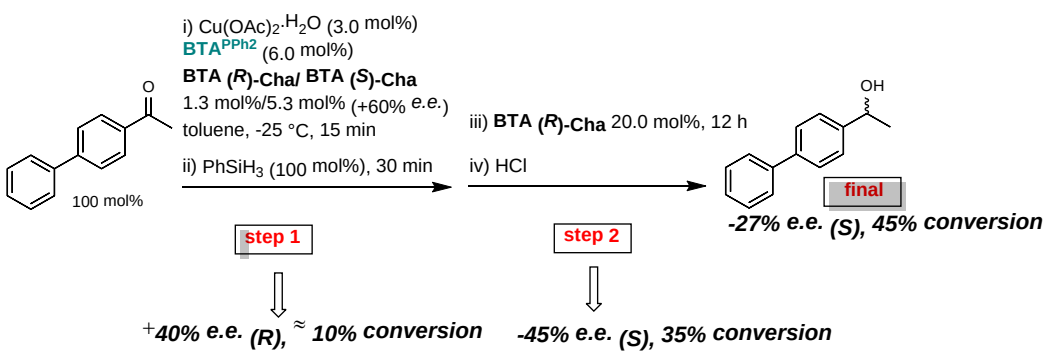

Reaction conditions: 1-(4-biphenylyl)ethanone (100 mol%), $Cu(OAc)_2 \cdot H_2O$ (3.0 mol%), **BTA^{PPh2}** (6.0 mol%), **BTA (*R*)-Cha/BTA (*S*)-Cha** (1.3 mol%/5.3 mol%, +60% *e.e.*), $PhSiH_3$ (100 mol%), toluene, -25 °C. **BTA (*R*)-Cha** (20.0 mol%) was added after 30 minutes**.** The conversion was determined by GC and ^1H NMR analyses. For the chiral HPLC analyses of step 1 (aliquot) and at the end of the reaction, see page S.28.

[a] The selectivity for step 2 was calculated according to the selectivities and conversions obtained in step 1 and at the end of the reaction. The selectivity of step 2 is optimal and inversed compared to step 1 confirming that full stereochemical switch occurs during the hydrosilylation of 1-(4-biphenylyl)ethanone.

Table S.5 Copper-catalysed hydrosilylation of 1:1 mixture of 1-(4-nitrophenyl)ethanone and 1-(4-biphenylyl)ethanone.[a]

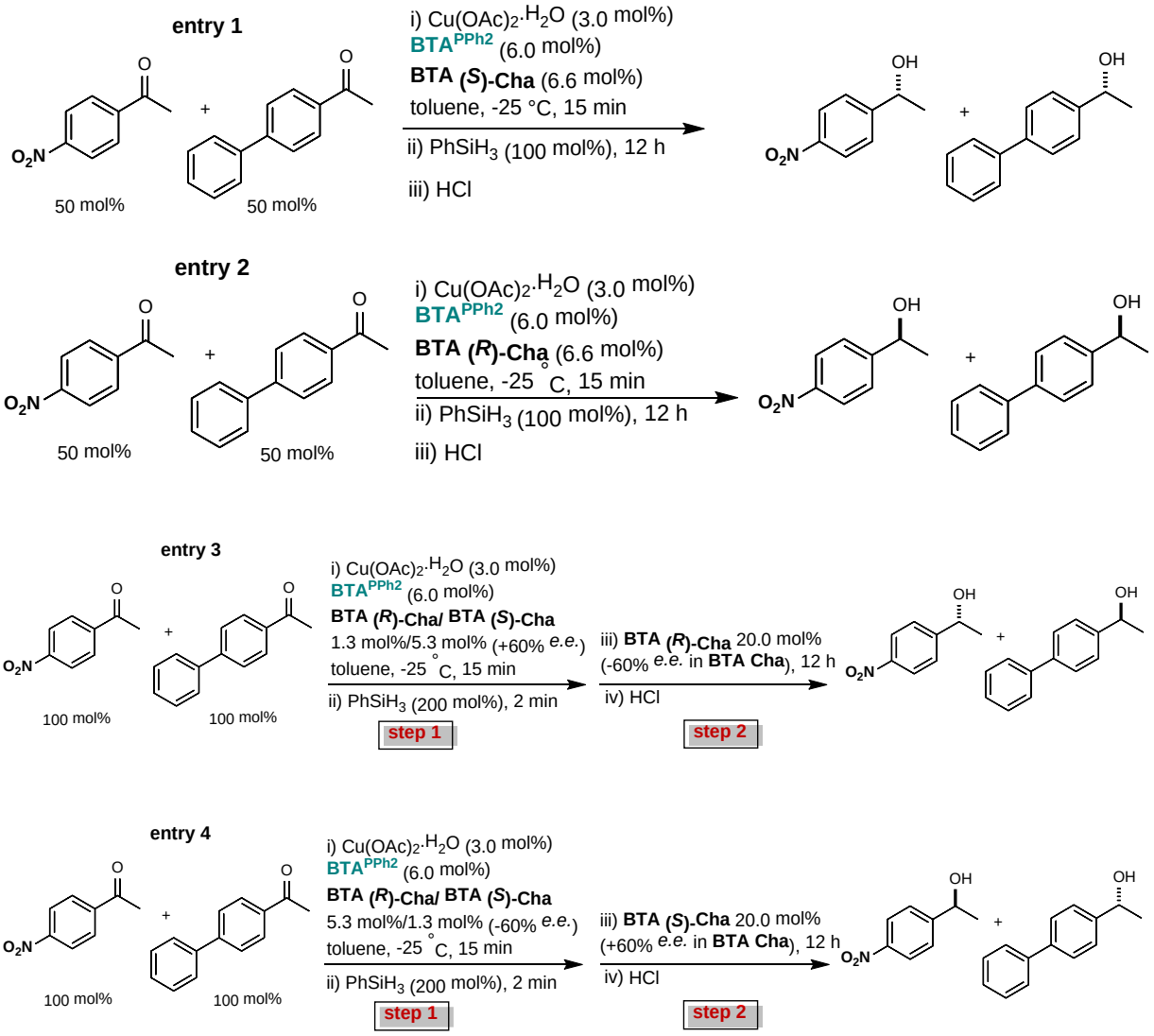

	1st step		2nd step		*e.e.* (%)	
Entry	**BTA (*R*)-Cha** (mol%)	**BTA (*S*)-Cha** (mol%)	**BTA (*R*)-Cha** (mol%)	**BTA (*S*)-Cha** (mol%)	**4-NO$_2$**	**4-Ph**
1	**BTA (*S*)-Cha** (6.6)				+77 (*R*)	+38 (*R*)
2	**BTA (*R*)-Cha** (6.6)				-79 (*S*)	-45 (*S*)
3	1.3	5.3	21.3	5.3	+74 (*R*)	-34 (*S*)
4	5.3	1.3	5.3	21.3	-69 (*S*)	+30 (*R*)

[a] Reaction conditions: 1-(4-nitrophenyl)ethanone (50 mol%, entries 1 and 2, 100 mol% entries 3 and 4), 1-(4-biphenylyl)ethanone (50 mol% entries 1 and 2, 100 mol% entries 3 and 4), $Cu(OAc)_2 \cdot H_2O$ (3.0 mol%), **BTA^{PPh2}** (6.0 mol%), enantiopure BTA Cha (entries 1 and 2) or **BTA (*R*)-Cha/BTA (*S*)-Cha** (**|*e.e.*| = 60 %, entries 3 and 4**), $PhSiH_3$ (100 mol% entries 1-2, 200 mol% entries 3-4), toluene, -25 °C. For the exact amount of BTA Cha present in each step, see the table. The conversion was determined by GC and ^1H NMR analyses. Conversion of 1-(4-nitrophenyl)ethanone was superior to 99% for all entries. Conversion of 1-(4-biphenylyl)ethanone was of 84% and 60% for entries 3 and 4 respectively. The optical purity of 1-(4-nitrophenyl)ethanol and 1-(4-biphenylyl)ethanol was determined by chiral GC and chiral HPLC analyses, respectively. For chiral GC analyses of entries 1-4, see pages S.30 and S.31.

General Procedures.

Preparation of new compounds**:** The synthetic procedure for the preparation of **BTA^{PPh2}** is detailed below. N,N-dimethylaminopyridine (DMAP), N-(3-dimethylaminopropyl)-N′-ethylcarbodiimide hydrochloride (EDC·HCl), phenylsilane, $Cu(OAc)_2 \cdot H_2O$, 1-(4-nitrophenyl)ethanone and 1-(4-biphenylyl)ethanone were acquired from commercial suppliers and used directly. 3,5-bisoctylaminocarbonyl-benzoic acid,[6] 4-diphenylphosphinoaniline,[7] **BTA (*S*)-Val**,[4] **BTA (*S*)-Tle**,[4] **BTA (*S*)-Leu**,[4] **BTA (*S*)-Ile**,[4] **BTA (*S*)-Cha**[3b] and **BTA (*R*)-Cha**[3b] were prepared following published procedures. Racemic phenyl alcohols were prepared by reduction of the corresponding aromatic ketones with $NaBH_4$ in methanol. Solvents for catalytic experiments were obtained from an SPS solvent purification system (IT-Inc). Chromatography-grade solvents were used for samples analysed by FT-IR and CD spectroscopy. NMR spectra were recorded on a Bruker Avance 300 spectrometer and calibrated to the residual solvent peak: DMSO-d_6 (^{1}H: 2.50 ppm; ^{13}C: 39.52 ppm). Peaks are reported with their corresponding multiplicity (s: singlet; d: doublet, t: triplet; m: multiplet) and integration, and respective *J* coupling constants are given in Hertz. Exact mass measurements (HRMS) were obtained on TQ R30-10 HRMS spectrometer by ESI+ ionization and are reported in m/z for the major signal.

Chiral GC and HPLC analyses: **1-(4-nitrophenyl)ethanol**. The optical purity was determined by GC analysis: Chiral Cyclosil-B column, 30 m × 250 µm x 0.25 µm, inlet pressure = 12.6 psi. Injection temperature = 220°C; detector temperature = 300°C; column temperature = 165°C. Retention time: 8.6 min (1-(4-nitrophenyl)ethanone), 18.9 min ((*R*)-enantiomer), 19.3 min ((*S*)-enantiomer).[8] **1-(4-biphenylyl)ethanol**. The optical purity was determined by HPLC analysis: Chiralpak AD-H column, heptane/isopropanol 97/3, flow=1 mL.min^{-1}, detection at 254 nm. Retention time: 17.8 min ((*S*)-enantiomer) and 20.2 min ((*R*)-enantiomer).[9] **Mixture of 1-(4-nitrophenyl)ethanol and 1-(4-biphenylyl)ethanol**. GC analysis: Chiral Cyclosil-B column, 30 m × 250 µm x 0.25 µm, inlet pressure = 12.6 psi. Injection temperature = 220°C; detector temperature = 300°C; column temperature = 165°C for 25 min, then 180°C for 20 min. Retention time: 18.9 min (1-(4-nitrophenyl)ethanol, (*R*)-enantiomer), 19.3 min (1-(4-nitrophenyl)ethanol, (*S*)-enantiomer), 29.6 min (1-(4-biphenylyl)ethanol, (*R*)-enantiomer), 29.9 min (1-(4-biphenylyl)ethanol, (*S*)-enantiomer).

Preparation of BTA solutions for analyses: the desired BTA was weighed into a ø11.6 mm HPLC vial or a ø20 mm glass vial, the volume of solvent was adjusted to the desired end

concentration with an adequate glass microsyringe, and verified by weighing the sample. Vials were sealed with PTFE-coated caps to avoid contamination from leaching plasticizer.

Fourier-Transform Infrared (FT-IR) analyses: FT-IR measurements were performed on a Nicolet iS10 spectrometer. Solution spectra were measured in CaF_2 cells by adjusting the pathlength (0.1 cm or 0.05 cm) to the concentration and were corrected for air, solvent and cell absorption.

Circular dichroism (CD) analyses: CD measurements were performed on a Jasco J-1500 spectrometer equipped with a Peltier thermostated cell holder and Xe laser. Data were recorded at 20°C with the following parameters: 20 $nm.min^{-1}$ sweep rate, 0.1 nm data pitch, 2.0 nm bandwidth, and between 400 and 200 nm. Spectra were corrected for solvent and cell contribution. A 0.1 mm dismountable quartz cell (2×10^{-3} M) was used. For all samples, LD contribution was negligible ($\Delta LD < 0.005$ dOD) and the shape of the CD signal was independent of the orientation of the quartz slide.

UV-Vis analyses: UV-Vis absorption spectra were extracted from CD on each of the above samples and obtained after correction of the absorption of air, solvent, and cell at the same temperature.

Small-angle neutron scattering (SANS) analyses: SANS measurements were made at the LLB (Saclay, France) on the PA20 instrument, at two distance-wavelength combinations to cover the 4.2×10^{-3} to $0.25 Å^{-1}$ q-range, where the scattering vector q is defined as usual, assuming elastic scattering, as $q=(4\pi/\lambda)\sin(\theta/2)$, where θ is the angle between incident and scattered beam. Data were corrected for the empty cell signal and the solute and solvent incoherent background. A light water standard was used to normalize the scattered intensities to cm^{-1} units.

Synthetic procedures.

Synthesis of **BTA^{PPh2}**: 3,5-bisoctylaminocarbonyl-benzoic acid[6] (1.50 g, 3.5 mmol) and dry THF (100 mL) were mixed in an oven-dried Schlenk flask under argon and then N,N-dimethylaminopyridine (0.72 g, 5.9 mmol), N-(3-Dimethylaminopropyl)-N′-ethylcarbodiimide hydrochloride (1.13 g, 5.9 mmol) and 4-diphenylphosphinoaniline[7] (1.44 g, 5.2 mmol) were added as solids. The reaction mixture was refluxed for 2 days. After cooling to room temperature, the mixture was evaporated under vacuum and the crude product was purified by column chromatography on silica gel eluting with DCM/AcOEt (95/5 to 7/1) to yield **BTA^{PPh2}** (1.90 g, 79%) as a colourless solid. **^{1}H NMR** (300 MHz, DMSO-d_6) δ 10.62 (s, 1H), 8.68 (t, *J* = 5.6 Hz, 2H), 8.45 (dd, *J* = 7.7, 1.6 Hz, 3H), 7.84 (d, *J* = 8.1 Hz, 2H), 7.46-7.37 (m, 6H), 7.31-7.21 (m, 6H), 3.29-3.22 (m, 4H), 1.61-1.47 (m, 4H), 1.36-1.11 (m, 20H), 0.90-0.79 (m, 6H). **^{31}P{^{1}H} NMR** (122 MHz, DMSO-d_6) δ -7.7. **^{13}C{^{1}H} NMR** (75 MHz, DMSO-d_6) δ 165.2, 165.0, 139.9, 137.0 (d, *J* = 11.4 Hz), 135.2, 135.1, 134.1 (d, *J* = 20.6 Hz), 133.1 (d, *J* = 19.4 Hz), 129.0, 128.9, 128.8, 128.7 (d, *J* = 6.8 Hz), 120.4 (d, *J* = 7.4 Hz), 39.6 (below the solvent peak), 31.3, 29.0, 28.8, 28.7, 26.5, 22.1, 13.9. **HRMS**: Calculated for $C_{43}H_{55}N_3O_3P$ $[M+H]^+$: 692.3976, found: 692.3973.

Catalytic experiments.

Catalytic screening (Tables 1 and S.1): An oven-dried test tube was loaded with $Cu(OAc)_2 \cdot H_2O$ (1.0 mg, 3.0 mol%) and **BTA^{PPh2}** (6.9 mg, 6.0 mol%) in dry THF (500 µL) and the mixture was stirred for 30 minutes. The solvent was removed under vacuum and the test tube was further put under vacuum (1.10^{-3} mbar) for 1 hour. 1-(4-nitrophenyl)ethanone (28.0 mg, 0.17 mmol) was added before flushing the tube with argon for 10 seconds. The BTA co-monomer (6.6 mol% in 200 µL of dry toluene) was added to the test tube as well as dry toluene in order to get a total volume of 590 µL. The mixture was stirred for 15 min at room temperature. $PhSiH_3$ (21.0 µL, 0.17 mmol) was added to the test tube and the mixture was stirred for 17 hours. Typical work-up: Aqueous solution of HCl (10 wt%, 400 µL) was added and the mixture was stirred for 30 min (until the solution became transparent). Then, the products were extracted with Et_2O (3x1 mL) and AcOEt (1x1 mL) and the solvents were evaporated under vacuum. The residue was taken up in DCM and passed through a silica plug eluting with DCM. The solvents were evaporated and the conversion and enantioselectivity were determined by ^1H NMR and chiral GC respectively.

Screening for chirality amplification (Table S.2): An oven-dried test tube was loaded with $Cu(OAc)_2 \cdot H_2O$ (1.0 mg, 3.0 mol%) and **BTA^{PPh2}** (6.9 mg, 6.0 mol%) in dry THF (500 µL) and the mixture was stirred for 30 minutes. The solvent was removed under vacuum and the test tube was further put under vacuum (1.10^{-3} mbar) for 1 hour. 1-(4-nitrophenyl)ethanone (28.0 mg, 0.17 mmol) was added before flushing the tube with argon for 10 seconds. A 25% *e.e.* scalemic mixture biased in favour of **BTA (*R*)-Cha** (x mol%) in 200 µL of toluene was added to the test tube as well as dry toluene in order to get a total volume of 590 µL. The mixture was stirred for 15 min at room temperature. The mixture was cooled to the desired temperature and further stirred for 15 min. $PhSiH_3$ (21.0 µL, 0.17 mmol) was added to the test tube and the mixture was stirred until completion of the reaction. The typical work-up procedure was followed.

Chirality amplification effect under optimized conditions (Figure 1a): An oven-dried test tube was loaded with $Cu(OAc)_2 \cdot H_2O$ (1.0 mg, 3.0 mol%) and **BTA^{PPh2}** (6.9 mg, 6.0 mol%) in dry THF (500 µL) and the mixture was stirred for 30 minutes. The solvent was removed under vacuum and the test tube was further put under vacuum (1.10^{-3} mbar) for 1 hour. 1-(4-nitrophenyl)ethanone (28.0 mg, 0.17 mmol) was added before flushing the tube with argon for 10 seconds. A scalemic mixture of **BTA Cha** (25.8 mg, 13.2 mol%, x% *e.e.*) in 200 µL of toluene was added to the test tube as well as dry toluene in order to get a total volume of 590

µL. The mixture was stirred for 15 min at room temperature. The mixture was cooled to 0 °C and further stirred for 15 min. $PhSiH_3$ (21.0 µL, 0.17 mmol) was added to the test tube and the mixture was stirred until completion of the reaction. The typical work-up procedure was followed.

Hydrosilylation of 1-(4-nitrophenyl)ethanone with sequential additions of substrate and $PhSiH_3$ (Table S.3, Figures 1b and S.10): A Schlenk tube tube was loaded with $Cu(OAc)_2 \cdot H_2O$ (1.0 mg, 3.0 mol%) and **BTA^{PPh2}** (6.9 mg, 6.0 mol%) in dry THF (500 µL) and the mixture was stirred for 30 minutes. The solvent was removed under vacuum and the Schlenk tube was further put under vacuum (1.10^{-3} mbar) for 1 hour. Then 1-(4-nitrophenyl)ethanone (28.0 mg, 0.17 mmol) was added before flushing the tube with argon for 10 seconds. **BTA (*R*)-Cha** (8.6 mg, 4.4 mol%) and **BTA (*S*)-Cha** (17.2 mg, 8.7 mol%) in 80 µL of dry toluene was added to the Schlenk tube as well as dry toluene in order to get a total volume of 590 µL. The mixture was stirred for 15 min at room temperature. The mixture was cooled to 0 °C and further stirred for 15 min. $PhSiH_3$ (42.0 µL, 0.34 mmol) was added and the mixture was stirred for 15 minutes. An aliquot was taken up, hydrolyzed with aqueous HCl and analyzed by chiral GC (*run 1*). Then, **BTA (*R*)-Cha** (25.4 mg, 13.0 mol%) in 200 µL of toluene was added and the mixture was stirred for 30 min before addition of 1-(4-nitrophenyl)ethanone (28.0 mg, 0.17 mmol) and $PhSiH_3$ (21.0 µL, 0.17 mmol). The mixture was stirred for 60 minutes and an aliquot was taken up, hydrolyzed with aqueous HCl and analyzed by chiral GC (*run 2*). Then, **BTA (*S*)-Cha** (50.7 mg, 26.0 mol%) in 100 µL of toluene was added and the mixture was stirred for 30 min before addition of 1-(4-nitrophenyl)ethanone (28.0 mg, 0.17 mmol) and $PhSiH_3$ (21.0 µL, 0.17 mmol). The mixture was stirred for 60 minutes and an aliquot was taken up, hydrolyzed with aqueous HCl and analyzed by chiral GC (*run 3*). Then, **BTA (*R*)-Cha** (100.0 mg, 52.0 mol%) in 200 µL of toluene was added and the mixture was stirred for 30 min before addition of 1-(4-nitrophenyl)ethanone (28.0 mg, 0.17 mmol) and $PhSiH_3$ (21.0 µL, 0.17 mmol). The mixture was stirred for 60 minutes and the typical work-up procedure was followed (*run 4*).

Table S.6 Determination of the enantiomeric excess in 1-(4-nitrophenyl)ethanol for each run of for the sequential copper-catalysed hydrosilylation of 1-(4-nitrophenyl)ethanone.

run	*e.e.*from the aliquots[a]	eq. of (*R*)/(*S*) product[b]	*e.r.* for the run	*e.e.* for the run
1	53%	0.765/0.235	76.5/23.5	53%
2	-2%	0.984/1.016	22.0/78.0	-56%
3	17%	1.75/1.25	76.5/23.5	53%
4	-1%	1.99/2.01	24.0/76.0	-52%

[a] "Cumulated" *e.e.* in 1-(4-nitrophenyl)ethanol (determined from the aliquots) for the different run, full conversion for each run. [b] "Cumulated" equivalents in (*R*) and (*S*) 1-(4-nitrophenyl)ethanol for the different run (100 mol% of 1-(4-nitrophenyl)ethanone is converted by run).

GC analyses From the aliquots of the different run**.**

Tables S.3, run 1:

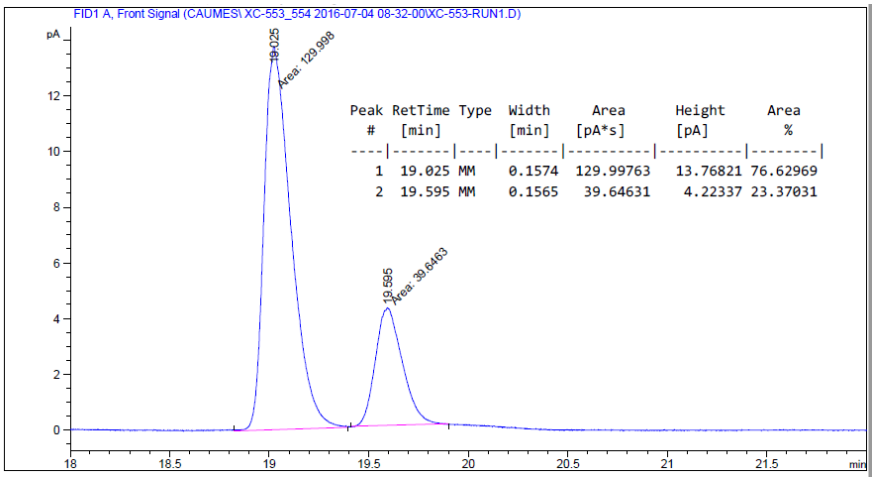

Tables S.3, run 2:

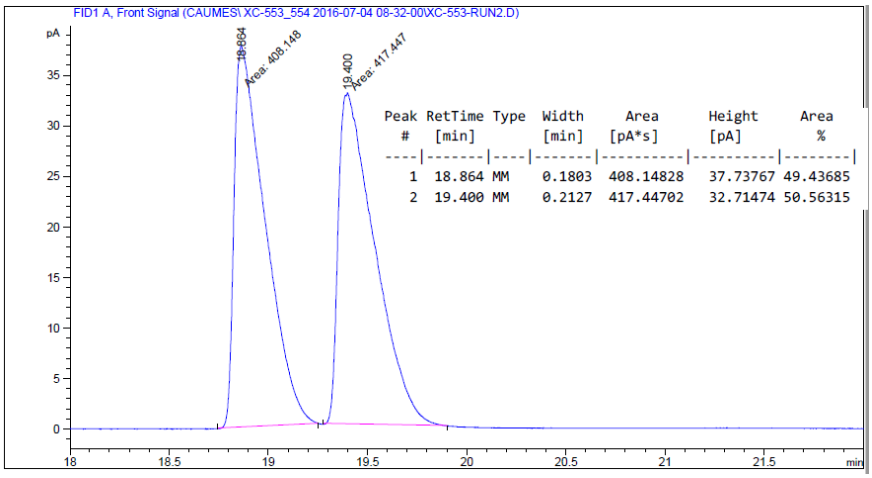

Tables S.3, run 3:

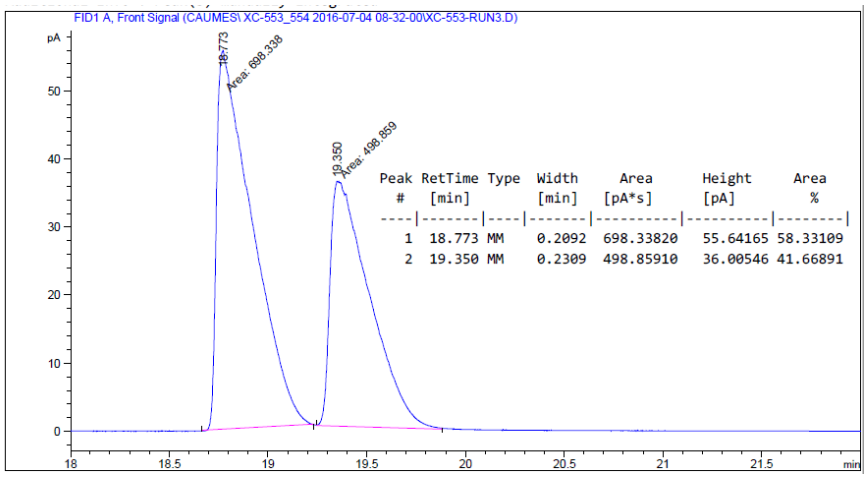

Tables S.3, run 4:

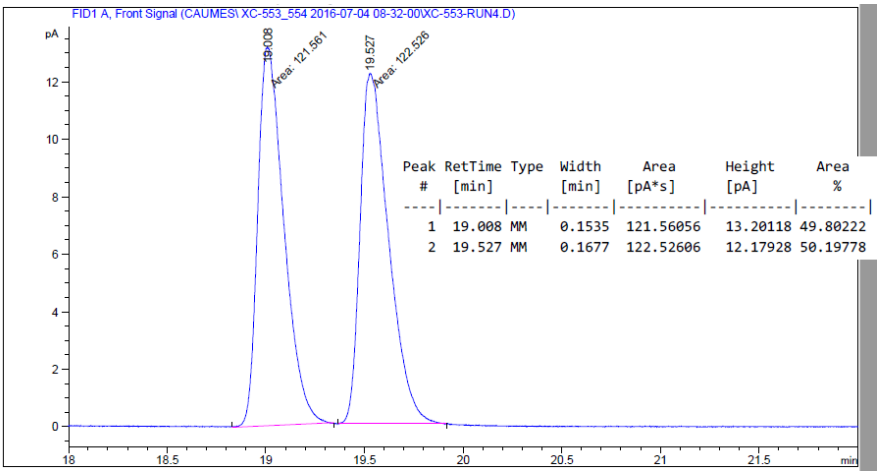

Determination of the time required for the stereochemical switch (Table S.4): A test tube was loaded with $Cu(OAc)_2 \cdot H_2O$ (1.0 mg, 3.0 mol%) and **BTA^{PPh2}** (6.9 mg, 6.0 mol%) in dry THF (500 µL) and the mixture was stirred for 30 minutes. The solvent was removed under vacuum and the test tube was further put under vacuum (1.10^{-3} mbar) for 1 hour. Then 1-(4-nitrophenyl)ethanone (28.0 mg, 0.17 mmol) was added before flushing the tube with argon for 10 seconds. **BTA (*R*)-Cha** (8.6 mg, 4.4 mol%) and **BTA (*S*)-Cha** (17.2 mg, 8.7 mol%) in 80 µL of dry toluene was added to the test tube as well as dry toluene in order to get a total volume of 590 µL. The mixture was stirred for 15 min at room temperature. The mixture was cooled to 0 °C and further stirred for 15 min. **BTA (*R*)-Cha** (25.4 mg, 13.0 mol%) in 200 µL of toluene was added as well as $PhSiH_3$ (21.0 µL, 0.17 mmol) after a measured time. The mixture was stirred for 10 minutes and the typical work-up procedure was followed.

GC analyses

Tables S.4, no switch: + 60% *e.e.(R)*

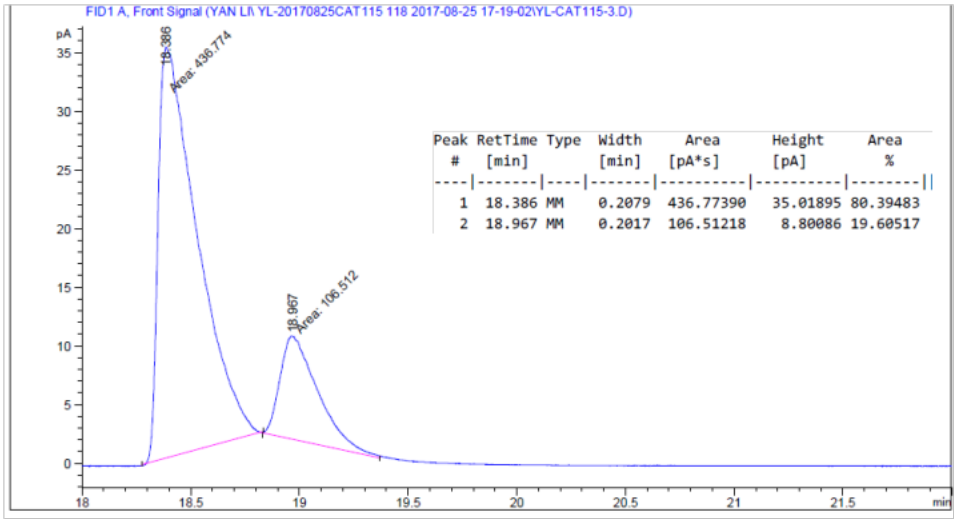

Tables S.4, entry 2 (5 seconds): -56% *e.e.(S)*

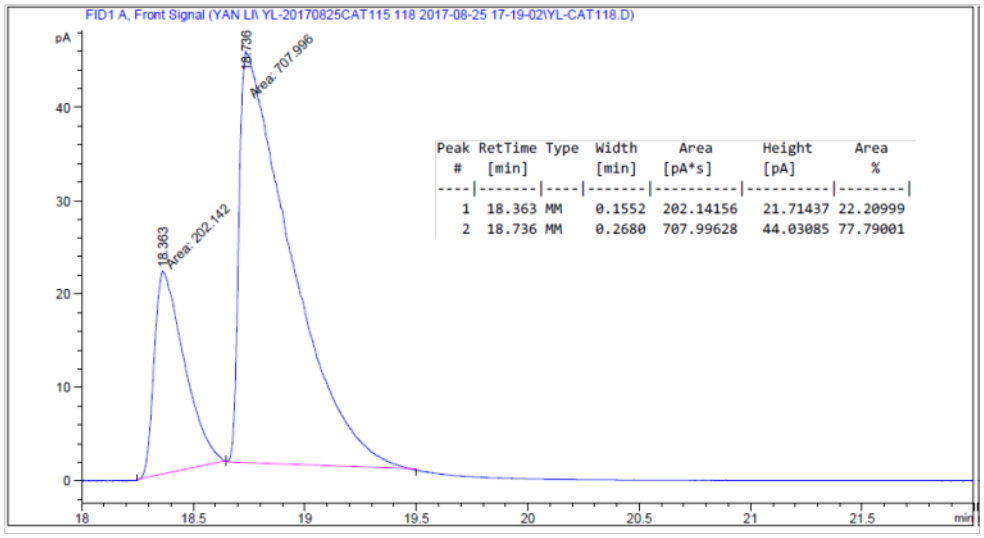

Stereochemical switch during the conversion of 1-(4-biphenylyl)ethanone (Scheme S.1a): A test tube was loaded with $Cu(OAc)_2 \cdot H_2O$ (1.0 mg, 3.0 mol%) and **BTA^{PPh2}** (6.9 mg, 6.0 mol%) in dry THF (500 µL) and the mixture was stirred for 30 minutes. The solvent was removed under vacuum and the test tube was further put under vacuum (1.10^{-3} mbar) for 1 hour. Then 1-(4-biphenylyl)ethanone (34.0 mg, 0.17 mmol) was added before flushing the tube with argon for 10 seconds. **BTA (*R*)-Cha** (8.6 mg, 4.4 mol%) and **BTA (*S*)-Cha** (17.2 mg, 8.7 mol%) in 80 µL of dry toluene was added to the test tube as well as dry toluene in order to get a total volume of 590 µL. The mixture was stirred for 15 min at room temperature. The mixture was cooled to 0 °C and further stirred for 15 min. Then, a solution of toluene (200 µL) containing **BTA (*R*)-Cha** (25.4 mg, 13.0 mol%) and $PhSiH_3$ (21.0 µL, 0.17 mmol) was added. The mixture was stirred for 3h and the typical work-up procedure was followed.

HPLC analyses

Scheme S.1a, no switch: + 34% *e.e.(R)*

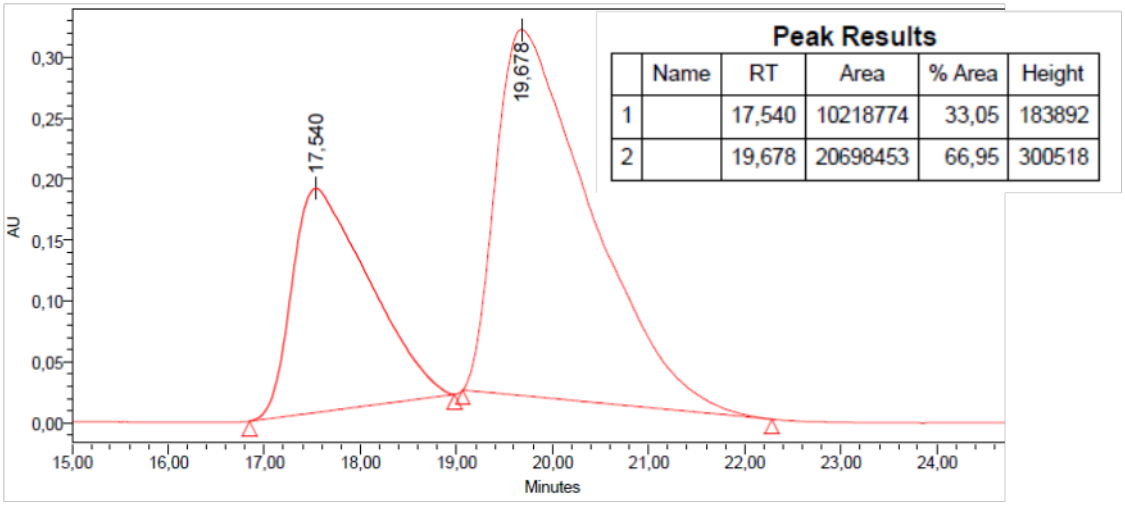

Scheme S.1a, switch: - 43% *e.e.(S)*

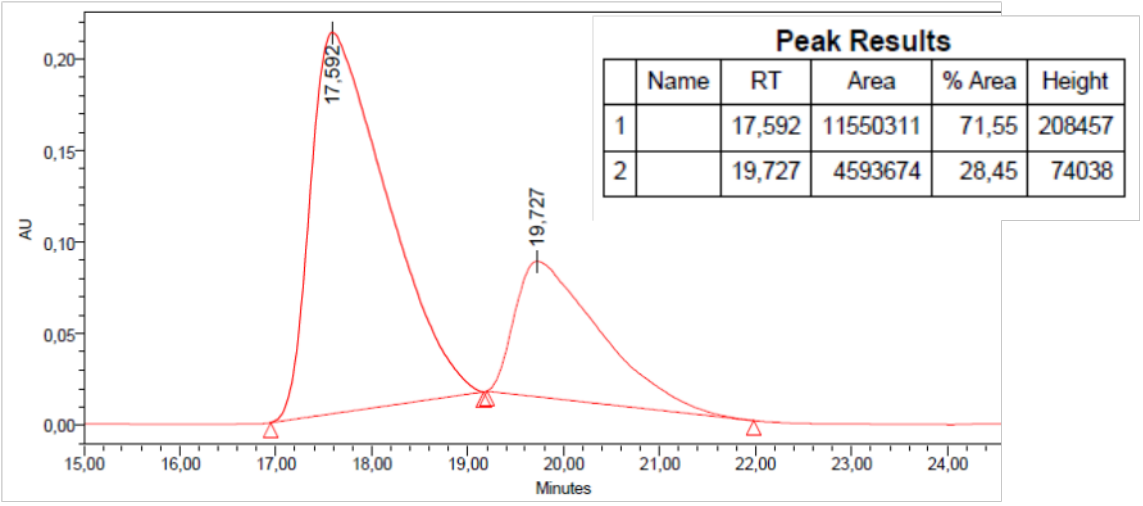

Stereochemical switch during the conversion of 1-(4-biphenylyl)ethanone (Scheme S.1b): A test tube was loaded with $Cu(OAc)_2 \cdot H_2O$ (1.0 mg, 3.0 mol%) and **BTA^{PPh2}** (6.9 mg, 6.0 mol%) in dry THF (500 µL) and the mixture was stirred for 30 minutes. The solvent was removed under vacuum and the test tube was further put under vacuum (1.10^{-3} mbar) for 1 hour. Then 1-(4-biphenylyl)ethanone (34.0 mg, 0.17 mmol) was added before flushing the tube with argon for 10 seconds. **BTA (*R*)-Cha** (2.6 mg, 1.3 mol%) and **BTA (*S*)-Cha** (10.3 mg, 5.3 mol%) in 80 µL of dry toluene was added to the test tube as well as dry toluene in order to get a total volume of 590 µL. The mixture was stirred for 15 min at room temperature. The mixture was cooled to -25 °C and further stirred for 15 min and then $PhSiH_3$ (21.0 µL, 0.17 mmol) was added. The mixture was stirred for 30 minutes, an aliquot was taken up and hydrolyzed (*step 1*) and **BTA (*R*)-Cha** (38.9 mg, 20.0 mol%) in 200 µL of toluene was added. The reaction mixture was stirred overnight and the typical work-up procedure was followed (*step 2*).

HPLC analyses

Scheme S.1b, aliquot (step 1): +40% *e.e. (R)*

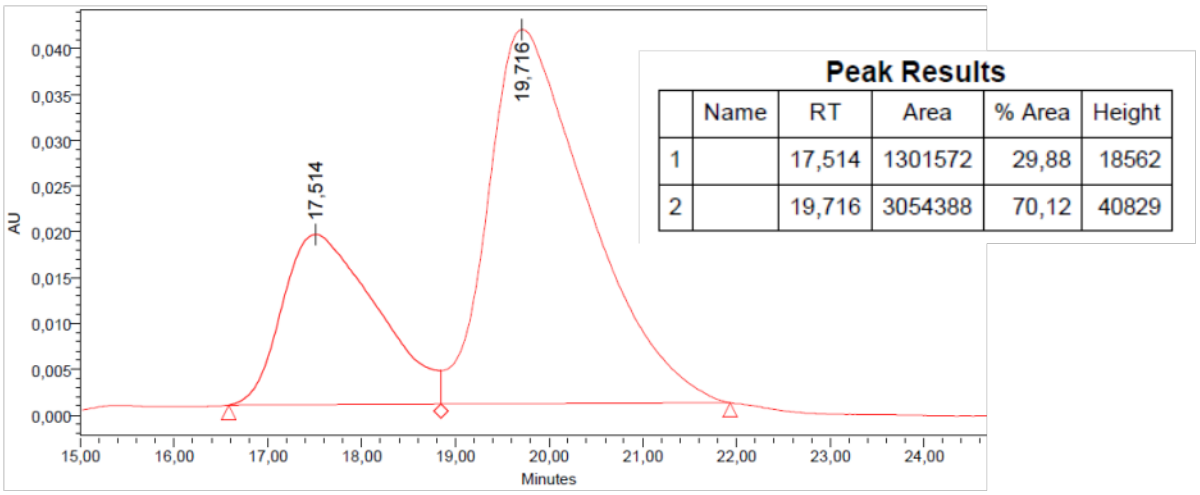

Peak Results

	Name	RT	Area	% Area	Height
1		17,514	1301572	29,88	18562
2		19,716	3054388	70,12	40829

Scheme S.1b, final: -27% *e.e (S)*

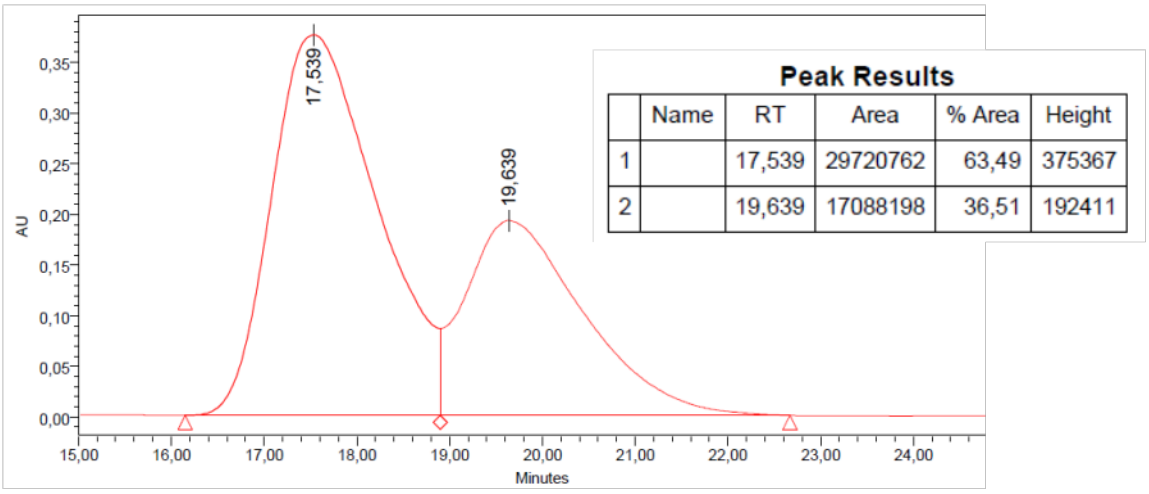

Peak Results

	Name	RT	Area	% Area	Height
1		17,539	29720762	63,49	375367
2		19,639	17088198	36,51	192411

Copper-catalysed hydrosilylation of 1:1 mixture of 1-(4-nitrophenyl)ethanone and 1-(4-biphenylyl)ethanone (Table S.5, Figure 1c): A Schlenk tube was loaded with $Cu(OAc)_2 \cdot H_2O$ (1.0 mg, 3.0 mol%) and **BTA^{PPh2}** (6.9 mg, 6.0 mol%) in dry THF (500 µL) and the mixture was stirred for 30 minutes. The solvent was removed under vacuum and the Schlenk tube was further put under vacuum (1.10^{-3} mbar) for 1 hour. 1-(4-nitrophenyl)ethanone (28.0 mg, 0.17 mmol) and 1-(4-biphenylyl)ethanone (34.0 mg, 0.17 mmol) were added before flushing the Schlenk tube with argon for 10 seconds. **BTA (*R*)-Cha** (2.6 mg, 1.3 mol%) and **BTA (*S*)-Cha** (10.3 mg, 5.3 mol%) in 200 µL of dry toluene was added to the Schlenk tube as well as dry toluene in order to get a total volume of 590 µL. The mixture was stirred for 15 min at room temperature. The mixture was cooled to -25 °C and further stirred for 15 min and then $PhSiH_3$ (42.0 µL, 0.34 mmol) was added. The mixture was stirred for 2 minutes (*step 1*) and then **BTA (*R*)-Cha** (38.9 mg, 20.0 mol%) in 200 µL of toluene was added. The reaction mixture was stirred for 12 h (*step 2*) and the typical work-up procedure was followed.

GC analyses. GC analyses below have been performed under conditions for which the enantiomers of 1-(4-nitrophenyl)ethanol and 1-(4-biphenylyl)ethanol are not perfectly separated, yet it indicated the configuration of the major enantiomer obtained and was thus a good demonstration of the success of the selectivity switch. The enantiomeric excesses (indicated above peaks) were precisely measured using adequate separation conditions for 1-(4-nitrophenyl)ethanol and 1-(4-biphenylyl)ethanol (page S.18). The peak at 26.8 min corresponds to 1-(4-biphenylyl)ethanone.

Table S.5, entry 1:

Peak #	RetTime [min]	Type	Width [min]	Area [pA*s]	Height [pA]	Area %
1	18.242	MF	0.2300	460.95221	33.40541	26.70793
2	18.841	FM	0.2372	75.29533	5.29038	4.36267
3	29.493	MF	0.1721	729.81598	70.69049	42.28611
4	29.759	FM	0.2324	459.83664	32.97412	26.64329

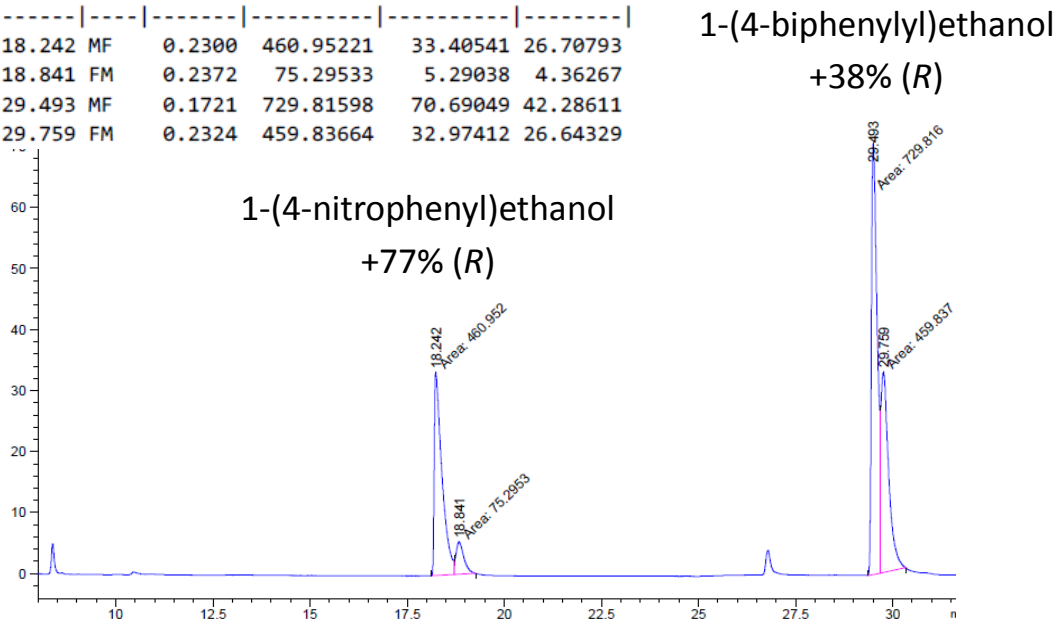

Table S.5, entry 2:

Peak #	RetTime [min]	Type	Width [min]	Area [pA*s]	Height [pA]	Area %
1	18.347	MM	0.1500	48.17480	5.35189	3.05227
2	18.716	MM	0.2320	415.54865	29.85732	26.32844
3	29.535	MF	0.1216	242.67874	33.25002	15.37570
4	29.728	FM	0.2286	871.92413	63.56655	55.24359

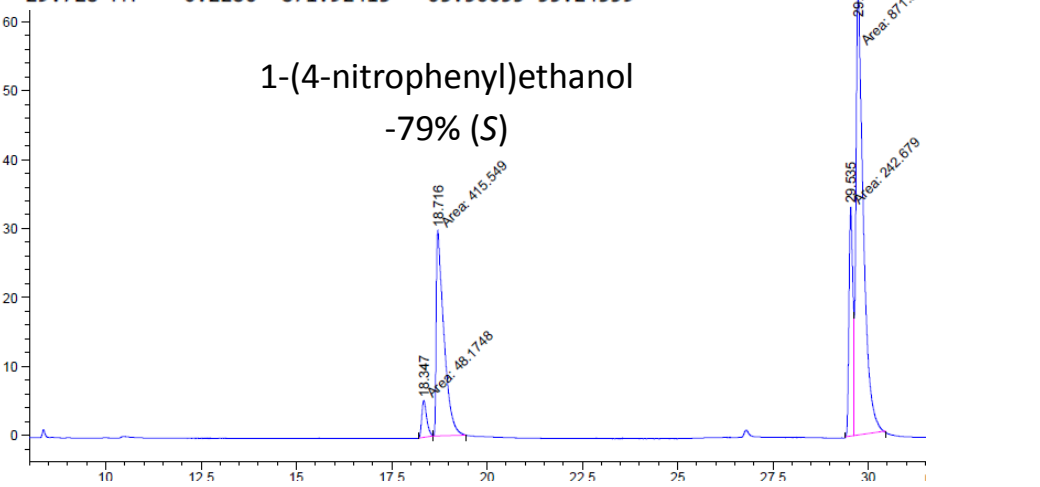

Table S.5, entry 3:

Peak #	RetTime [min]	Type	Width [min]	Area [pA*s]	Height [pA]	Area %
1	18.421	MM	0.1918	272.00754	23.63305	23.28780
2	18.986	MM	0.1799	41.17962	3.81563	3.52557
3	29.649	MF	0.1261	236.66132	31.28087	20.26165
4	29.853	FM	0.2130	618.17761	48.36099	52.92498

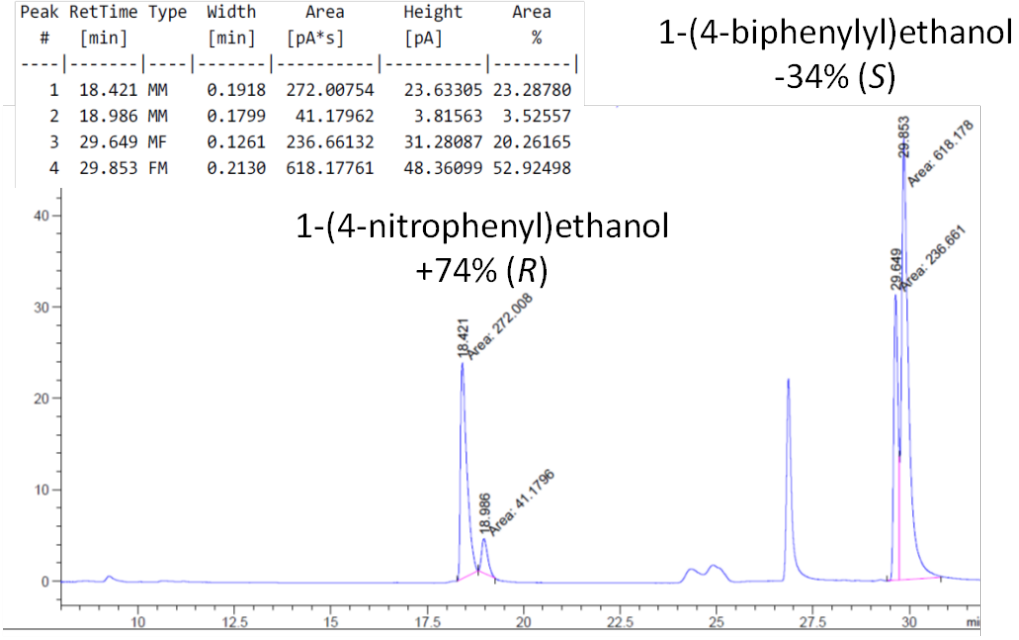

Table S.5, entry 4:

Peak #	RetTime [min]	Type	Width [min]	Area [pA*s]	Height [pA]	Area %
1	18.542	MM	0.1616	34.87117	3.59671	4.43060
2	18.979	MM	0.2011	187.59395	15.54638	23.83501
3	26.877	MM	0.1482	249.10402	28.01308	31.65025
4	29.694	MM	0.2670	315.48309	19.69057	40.08414

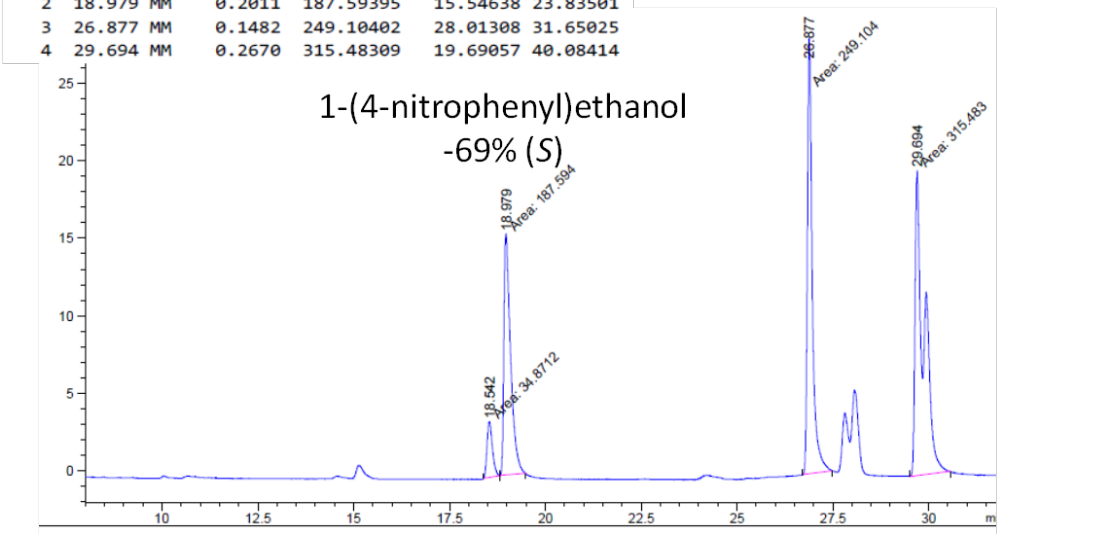

BTA^{PPh2}

^{1}H (DMSO-d$_6$):

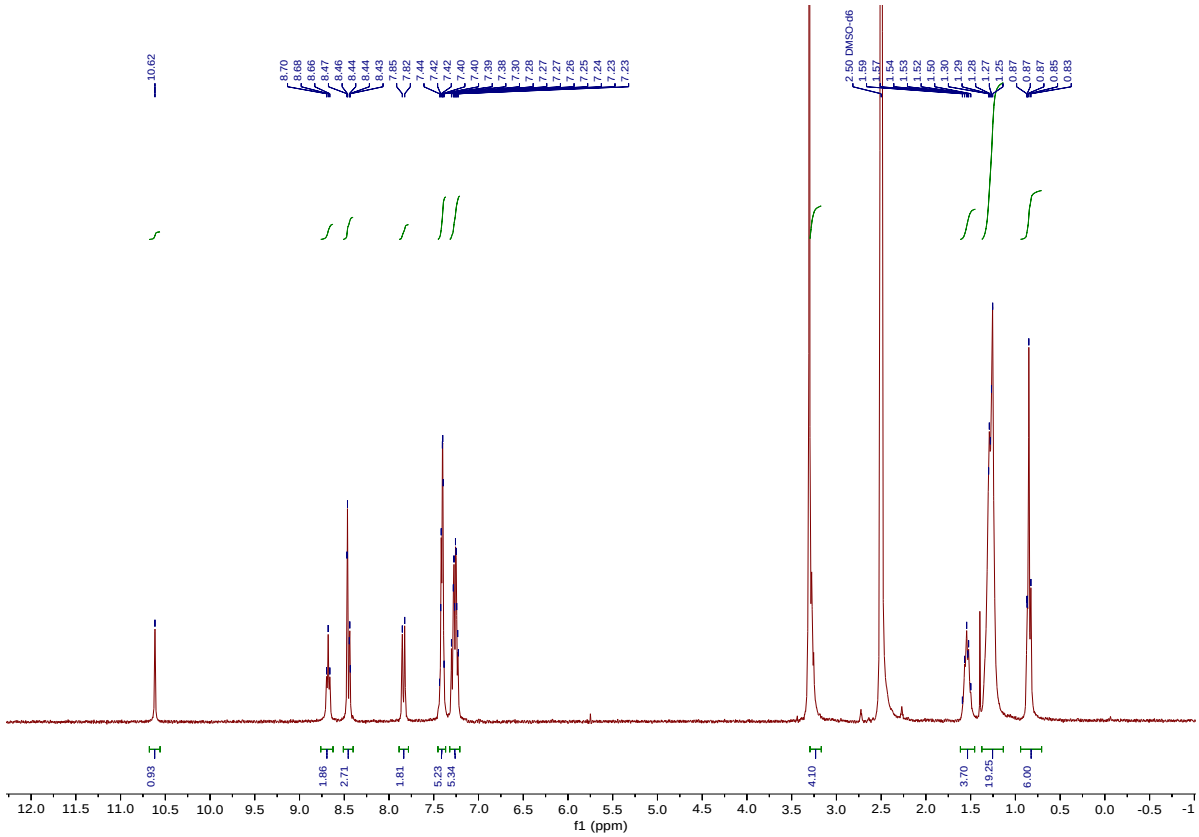

^{31}P{^{1}H} (DMSO-d$_6$):

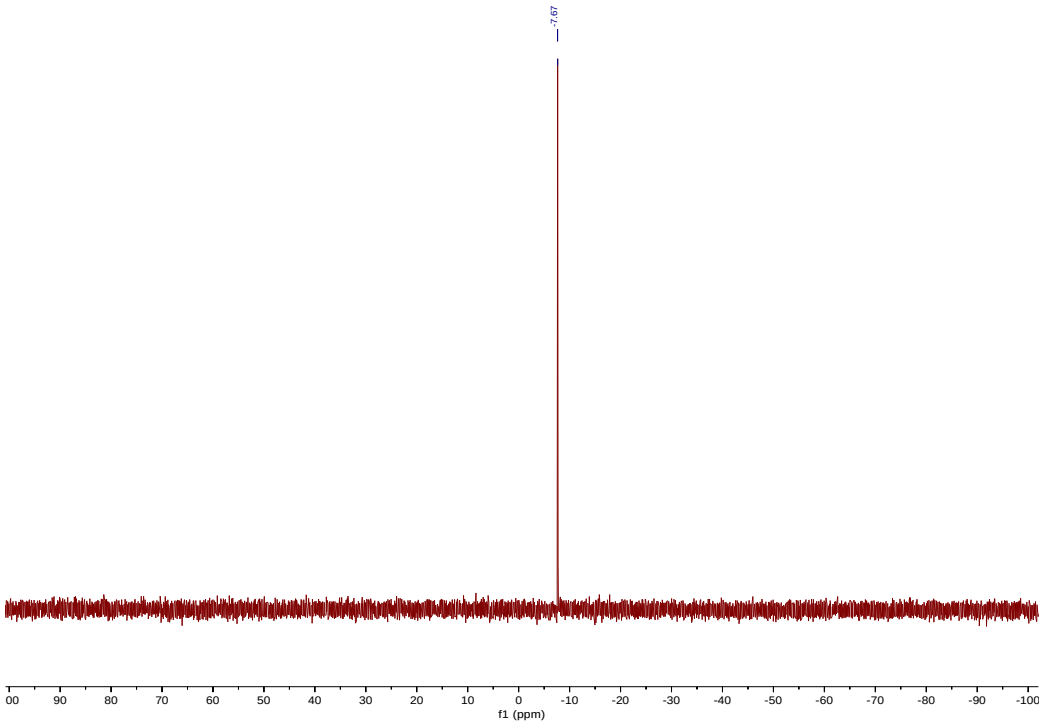

$^{13}C\{^{1}H\}$ (DMSO-d_6):

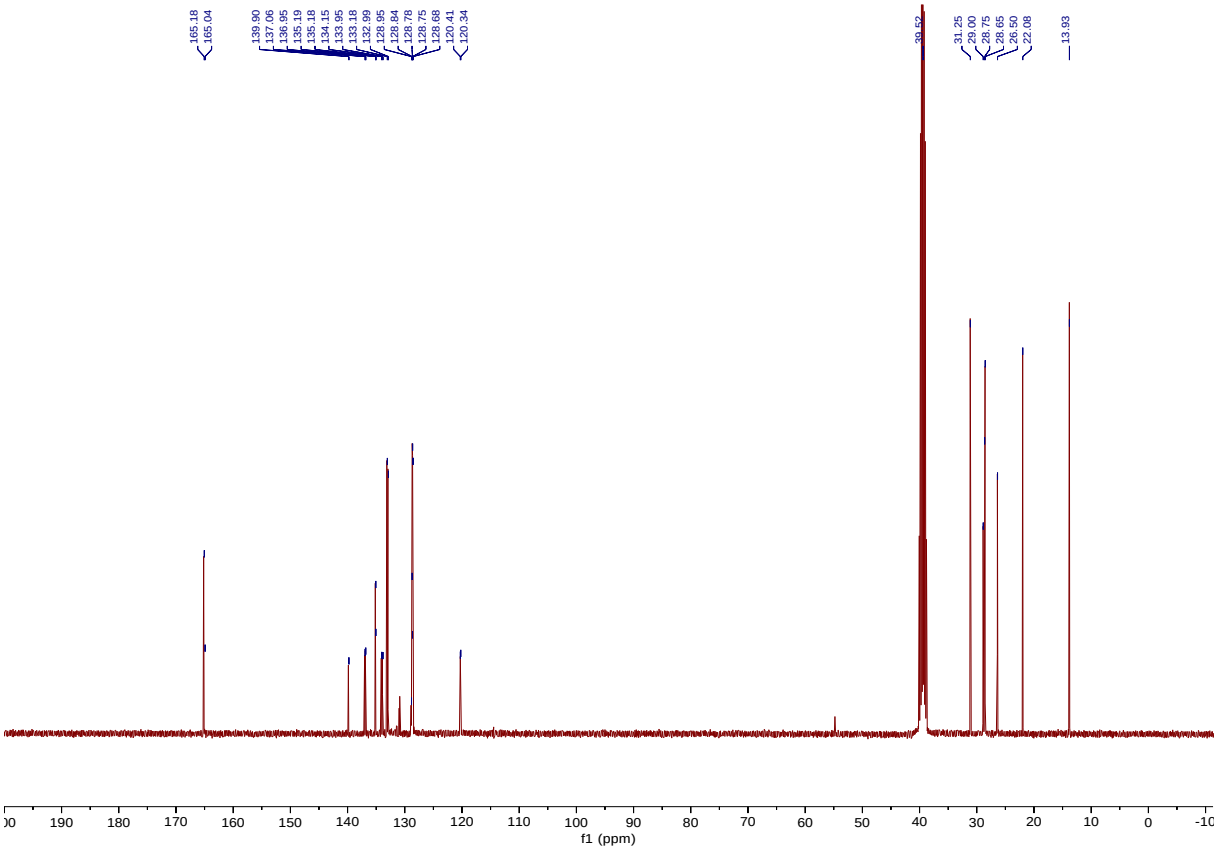

References:

[1] V. Simic, L. Bouteiller, M. Jalabert, *J. Am. Chem. Soc.* **2003**, *125*, 13148-13154.

[2] T. F. A. De Greef, M. M. J. Smulders, M. Wolffs, A. P. H. J. Schenning, R. P. Sijbesma, E. W. Meijer, *Chem. Rev.* **2009**, *109*, 5687-5754.

[3] a) A. Desmarchelier, M. Raynal, P. Brocorens, N. Vanthuyne, L. Bouteiller, *Chem. Commun.* **2015**, *51*, 7397-7400; b) A. Desmarchelier, B. Giordano Alvarenga, X. Caumes, L. Dubreucq, C. Troufflard, M. Tessier, N. Vanthuyne, J. Idé, T. Maistriaux, D. Beljonne, P. Brocorens, R. Lazzaroni, M. Raynal, L. Bouteiller, *Soft Matter* **2016**, *12*, 7824-7838; c) X. Caumes, A. Baldi, G. Gontard, P. Brocorens, R. Lazzaroni, N. Vanthuyne, C. Troufflard, M. Raynal, L. Bouteiller, *Chem. Commun.* **2016**, *52*, 13369-13372.

[4] A. Desmarchelier, X. Caumes, M. Raynal, A. Vidal-Ferran, P. W. N. M. van Leeuwen, L. Bouteiller, *J. Am. Chem. Soc.* **2016**, *138*, 4908-4916.

[5] S. Allenmark, *Chirality* **2003**, *15*, 409-422.

[6] J. Roosma, T. Mes, P. Leclère, A. R. A. Palmans, E. W. Meijer, *J. Am. Chem. Soc.* **2008**, *130*, 1120-1121.

[7] D. Gelman, L. Jiang, S. L. Buchwald, *Org. Lett.* **2003**, *5*, 2315-2318.

[8] G. Uray, W. Stampfer, W. M. F. Fabian, *J. Chromatogr. A* **2003**, *992*, 151-157.

[9] K. Junge, B. Wendt, D. Addis, S. L. Zhou, S. Das, M. Beller, *Chem. Eur. J.* **2010**, *16*, 68-73.